

Supporting Information for:

Identification of Thermal Conduits that Link the Protein-Water Interface to the Active Site Loop
and Catalytic Base in Enolase

Emily J. Thompson,^{1,2} Adhayana Paul,^{1,2} Anthony T. Iavarone,^{1,2} and Judith P. Klinman^{1,2,3}

1. Department of Chemistry, University of California, Berkeley, CA 94720, USA
2. California Institute for Quantitative Biosciences (QB3), University of California, Berkeley, CA 94720, USA
3. Department of Molecular and Cell Biology, University of California, Berkeley, CA 94720, USA

*Corresponding Author; email: klinman@berkeley.edu

Table of Contents

1. Materials and Methods	3
a. Materials.....	3
b. Enzymatic synthesis of potassium 2-phospho-D-glycerate.....	3
c. Enzymatic synthesis of potassium 2- ² H-2-phospho-D-glycerate.....	3
d. Instruments.....	3
e. Enolase protein expression and purification.....	3
f. Mutagenesis of enolase.....	3
g. Kinetics.....	4
h. Kinetic Isotope Effects.....	4
i. HDX sample preparation.....	4
j. HDX reproducibility.....	4
k. Peptide identification via liquid chromatography-tandem mass spectrometry.....	4
l. HDX measurements using liquid chromatography-mass spectrometry.....	5
m. HDX equilibrium sample preparation.....	5
n. HDX mass spectrometry raw data analysis.....	5
o. HDX peptide analysis.....	5
p. Thermal stability of enolase.....	6
q. Discussion of type II exceptions from $\Delta E_a(\text{HDX})$ table.....	6
2. Figures.....	6
3. Tables.....	12
4. HDX Uptake Plots.....	16
5. $E_{a\text{HDX}}$ Plots.....	24
6. References.....	28

1. Materials and Methods

a. Materials. All water (H₂O) was purified to a resistivity of 18.2 MΩ•cm (at 25 °C) using a Milli-Q Plus gradient ultrapure water purification system (Millipore). Potassium phosphoenolpyruvate was purchased from Cayman Chemical. Calcium DL-glycerate hydrate was purchased from TCI America. Deuterium oxide (D₂O, 99.9% D), lactate dehydrogenase from rabbit, pyruvate kinase from rabbit muscle, pepsin from porcine gastric mucosa, adenosine triphosphate, and sodium adenosine diphosphate were purchased from Sigma Aldrich. β-nicotinamide adenine dinucleotide reduced sodium salt hydrate was purchased from Roche Diagnostics. Q5 Master Mix, DpnI, T4 polynucleotide kinase, T4 DNA ligase, and prestained protein ladder standard were purchased from New England Biolabs. Mini-PROTEAN® TGX™ gels were purchased from Bio-Rad. Competent cells were purchased from the University of California, Berkeley MacroLab.

b. Enzymatic synthesis of potassium 2-phospho-D-glycerate. At the time of these studies, potassium 2-phospho-D-glycerate (2-PGA) was not readily commercially available in good purity. 2-PGA was enzymatically synthesized from glycerate-2-kinase (G2K) based on a literature procedure with minor modification.¹ The G2K plasmid was obtained from Paul A. Sims and expressed and purified. The purity was checked using SDS-Page. The synthesis of 2-PGA was carried out according to the literature. The purification of 2-PGA was based on the literature with modifications as outlined herein. Instead of an activated charcoal column, the reaction mixture was stirred over activated charcoal for 10 minutes and then filtered through a medium porosity glass frit, resulting in an A₂₆₀ corrected for dilution of ~3. A different volatile buffer, ammonium bicarbonate, was used for the successful elution of 2-PGA from the column. A peristaltic pump was used with the HCO₃⁻ anion exchange column at a flow rate of 2.5 mL min⁻¹ and collected in 6 mL fractions. To assay fractions, a coupled assay cocktail (440 μM NaADP, 90 μM NADH, 20 u/mL lactate dehydrogenase, 2.4 u/mL pyruvate kinase, and 0.02 μM enolase) was prepared and equal volumes of the cocktail and fractions were used. The absorbance of each fraction was recorded at 340 nm every five minutes. Fractions with a decrease in absorbance were collected and combined. The literature preparation was followed in all other steps. Identity and purity were confirmed by ¹H and ³¹P NMR.

c. Enzymatic synthesis of potassium 2-²H-2-phospho-D-glycerate. The deuterated substrate was synthesized according to the literature with variant Glu211Gln.² NMR was performed to confirm the deuteration.

d. Instruments. Neslab RTE-111 refrigerated bath recirculated chillers were used for hydrogen-deuterium exchange (HDX) measurements and all kinetic assays. Spectrophotometry was carried out on Cary 50 Bio and Cary 50 Scan UV-vis spectrophotometers. A Fisher Scientific Isotemp Incubator with an Innova 2000 benchtop shaker were used for small culture growth. An Innova 4400 incubated shaker was used for expressions. Circular dichroism was performed on an Aviv Biomedical, Inc. Circular Dichroism Spectrometer Model 410. Intact protein mass spectrometry was carried out on a Synapt G2-Si mass spectrometer (Waters, Milford, MA).

e. Enolase protein expression and purification. Enolase was expressed and purified according to the literature.³ Protein identity and purity were confirmed and assessed using SDS-PAGE and intact protein mass spectrometry (Figure S7). Typical yields were 70 mg of purified enolase per liter of culture.

f. Mutagenesis of enolase. Site-directed mutagenesis was carried out using the New England Biolabs Q5 system starting from the WT plasmid. The mutant plasmids were first isolated from XL-1 Blue cells and confirmed by sequencing using the T7 forward and T7 reverse primers by the

University of California, Berkeley DNA Sequencing Facility. Expression and purification for all mutants followed the same procedure as WT.

g. Kinetics. Steady-state kinetic assays were performed using direct assessment of the product formation (phosphoenolpyruvate) at 240 nm on a Cary 50 UV-vis spectrophotometer using the kinetics module (single-wavelength mode). Substrate concentrations were varied from 5-300 μM . Enzyme concentration varied with mutation; WT was assayed at 5 nM. The k_{cat} , K_M , and $^Dk_{\text{cat}}$ kinetic parameters were determined from non-linear fits in GraphPad Prism 8. The enthalpic barrier for catalysis, $E_a(k_{\text{cat}})$, was determined by linear fit of the Arrhenius plot from at least five temperatures. The data were also fit to the Eyring equation and plotted (Figure S11).

h. Kinetic Isotope Effects. The complexity of the chemical mechanism of enolase, as clearly laid out by Knowles and other investigators, is reflected in the variation of the primary kinetic isotope effect as a function of pH and Mg^{2+} ion concentration.⁴⁻⁶ Our approach was to search for which of the earlier papers reported KIEs that were collected under the conditions that were anticipated to be optimal for HDX experiments. We settled on the conditions of pH 7.5, 50 mM HEPES, and 2 mM Mg^{2+} , identical to the studies by Poyner et al.⁵ Experiments were conducted following the methodology outlined above, under conditions of saturating substrate where k_{cat} approaches V_{max} for WT and Leu343Ala at all temperatures.

i. HDX sample preparation. Samples were collected over 15 time points (0, 10, 20, 30, 45, 60, 180, 300, 600, 1800, 3600, 5400, 7200, 10800, 14400 seconds) and five temperatures (temperatures studied: 10, 20, 25, 30, 40 $^{\circ}\text{C}$). Aliquots of purified wild-type and variant enolase were prepared at 100 μM . 45 μL aliquots of D_2O buffer (10 mM HEPES, 2mM MgCl_2 , pD 7.5; corrected pD = $\text{pH}_{\text{read}} + 0.4$ (see literature⁷)) and enzyme were equilibrated separately at the given temperature before initiating the exchange experiment by adding 5 μL of enzyme to the D_2O buffer (a 10-fold dilution). Samples were incubated at a specified temperature for a given length of time and then quenched. To quench the reaction, samples were rapidly cooled for 5 s in a -10 $^{\circ}\text{C}$ ice bath and adjusted to pH 2.4 by addition of 20 μL of 0.32 M citric acid with 2 M guanidinium chloride. Pepsin (10 μL of 0.2 mg/mL) was then added and mixed. The sample was transferred to a 250 μL polypropylene insert tube (Agilent) and rested on ice for 2 minutes. Following, the sample was immediately flash frozen in liquid nitrogen and stored at -80 $^{\circ}\text{C}$ until mass spectrometry was conducted. A zero time point was also collected, where the protein was diluted 10-fold in an equivalent H_2O buffer (10 mM HEPES, 2 mM MgCl_2 , pH = 7.5) and immediately quenched and digested following the same procedure. Guanidinium chloride was added as a chaotropic agent and greatly increased the protein sequence coverage and the number and abundance of unique peptides. Pepsin and acid solutions were stored on ice to maintain a low temperature throughout the quenching and digestion process, to minimize back exchange.

j. HDX reproducibility. Time points were collected non-sequentially over three days to reduce systematic error and error induced from minor differences in peptide aliquots (day 1: 0, 30, 180, 1800, 7200 s; day 2: 10, 45, 300, 3600, 10800 s; day 3: 20, 60, 600, 5400, 14400 s). One data set is considered to be 15 time points at one temperature. Each data set was collected at least twice with different protein expressions to provide a biological replicate. While three replicates are generally recommended, the potential for systematic or random error is minimized by collecting two replicates over five temperatures and with collection over three days for each data set.

k. Peptide identification via liquid chromatography-tandem mass spectrometry. Samples of pepsin-digested proteins were analyzed using an UltiMate3000 RSLCnano liquid chromatography (LC) system that was connected in-line with an LTQ-Orbitrap-XL mass

spectrometer equipped with an electrospray ionization source (Thermo Fisher Scientific, Waltham, MA), as described.¹

l. HDX measurements using liquid chromatography-mass spectrometry. Deuterated, pepsin-digested protein samples from HDX experiments were analyzed using an Agilent 1200 LC system (Santa Clara, CA) that was connected in-line with the LTQ-Orbitrap-XL mass spectrometer (Thermo), as described.¹

m. HDX equilibrium sample preparation. A maximally labeled control sample was prepared by incubating lyophilized WT protein in 100% D₂O buffer at 90 °C for 2 hours. The sample was then treated the same as the time point samples, substituting H₂O buffer to dilute the sample to 90% D₂O before quenching and digestion. This data is used to calculate the back exchange occurring between the completion of HDX and the mass spectrometry measurement.

n. HDX mass spectrometry raw data analysis. Analysis of the mass spectrometry data is carried out in HDX Workbench⁸ and the data fitting and plotting is carried out through a Python workflow described in the next section. A non-overlapping set of peptides was chosen and curated (Figure S5, 31 unique peptides). Beyond peptide location in the sequence, peptides were chosen based on appearance in all data sets (WT and variants) and peptide resolution. A preference was also given for shorter peptides over longer lengths. For each data set, curation includes manual assessment of every peptide at every time point in HDX Workbench. Peptide chromatograms were checked and/or corrected as needed for identity, signal-to-noise ratios, EX1 or EX2 behavior, and overlap of similar eluting peptides. After each data set was checked, it was “finalized” in HDX Workbench and the XML file in the summaries folder was extracted for the next step of analysis.

o. HDX peptide analysis. Previous work in our group has focused on identifying temperature-dependent trends and current work is focused on quantifying the temperature-dependence trends seen in HDX through statistically robust methods.^{9,10} HDX-MS data are plotted as HDX in Daltons versus time in minutes and traces fit to three exponentials using Equation 1, which accounts for four types of amide exchange rates: fast exchange ($k_{\text{fast}} > 2.5 \text{ min}^{-1}$), medium exchange ($2.5 > k_{\text{med}} > 0.1 \text{ min}^{-1}$), slow exchange ($0.1 \text{ min}^{-1} > k_{\text{slow}}$), and non-exchanging ($k \cong 0$, within the experimental parameters):

$$\text{Daltons} = N_{\text{tot}} - Ae^{-k_{\text{fast}}t} - Be^{-k_{\text{med}}t} - Ce^{-k_{\text{slow}}t} - N_{\text{NE}} \quad (1)$$

where N_{tot} is the total number of amides that can exchange, N_{NE} is the total number of non-exchanging amides, and A, B, and C represent the total number of amides exchanging in the fast, medium, and slow rate regimes. Finally, a weighted average rate of exchange (k_{wa}) is defined, according to Equation 2:

$$k_{\text{wa}} = \frac{Bk_{\text{med}} + Ck_{\text{slow}}}{N_{\text{tot}}} \quad (2)$$

where the constants are as defined in Equation 1. k_{wa} excludes the k_{fast} parameter, which is outside the time frame observed in our experiments and generally too noisy to give rise to statistically relevant data. Each monitored rate constant, k_{med} and k_{slow} , is normalized by the fraction of amides exchanging in that time regime and is expected to vary with temperature as, for example, amides in the non-exchanging regime move into k_{slow} , and slowly exchanging amides contribute to k_{med} . To facilitate high-throughput analysis of the large amounts of data generated from the combination of temperature- and mutation-dependent HDX-MS experiments, a Python code was written and is available on GitHub.

We developed a workflow in Python (version 3.6) using Matplotlib, Pandas, and Seaborn to handle the large amount of data generated in these experiments.^{11,12} The workflow and code have been uploaded to GitHub (https://github.com/ejt-hdx/2020_HDX_eno).

- i. *Extract data from XML files.* Data from the HDX Workbench XML files were extracted and tabulated according to the start, end, sequence, temperature, time point, and replicate values.
 - ii. *Equilibrium sample correction.* The equilibrium back exchange data was extracted from the XML file as above, and then manually curated in Excel to make a table with only the non-overlapping peptide set. The tabulated data for the temperature-dependent data sets were merged with the back exchange table, dropping any peptide data that is not part of the chosen peptide set. The raw data is then corrected for back exchange according to the equation and discussion described above.
 - iii. *Fitting the data.* Data were fit using three exponentials as discussed in the main text. Trials with one and two exponentials were insufficient to fit the data across all peptides with a reasonable standard deviation of the residuals.
 - iv. *E_{aHDX} calculations.* E_{aHDX} was calculated as described in the main text and in the literature.⁹
 - v. *Graphing.* Data are graphed using Seaborn and Matplotlib. Both linear and semi-log plots were used to visually assess the temperature-dependent data.
- p. Thermal stability of enolase.** Circular dichroism was used to measure the approximate melting temperature of the native enolase and Leu343Ala. Experiments were conducted at 222 nm with 0.5 μ M enzyme in 25 mM Na_2HPO_4 buffer (pH 7.5) with 1.0 mM MgCl_2 . Experiments were run in a Starna Cells cuvette (21-Q-10/CD, 1-cm path length) with stirring. Data was collected between 25 $^\circ\text{C}$ and 97 $^\circ\text{C}$, at intervals of three degrees, equilibrating for five minutes at each temperature. The melting temperature was calculated from the first derivative of the curve and is the average of at least three experiments (Figure S9). WT enolase has a melting point of 46.4 $^\circ\text{C}$ and Leu343Ala has a melting point of 46.0 $^\circ\text{C}$.
- q. Discussion of type II exceptions from $\Delta E_a(\text{HDX})$ table.** All Type II peptides and their $E_a(\text{HDX})$ and $\Delta E_a(\text{HDX})$ values are shown in Table S6. Four peptides are excluded from Table 2 in the main text despite having $\Delta E_a(\text{HDX})$ values greater than their error (these are noted in Table S6). Peptide 138-152 only has four data points for the WT $E_a(\text{HDX})$ calculation and the removal of one terminal data point would make the WT and L343A lines parallel. Peptides 280-286 and 287-294 are short peptides and both the WT and L343A datasets exhibit very noisy k_{HDX} data, likely because the primary change in the k_{med} and k_{slow} rate constants is measuring just a single amide. Peptide 387-407 is also excluded due to the high level of noise. This peptide demonstrates behavior that is borderline Type I, making the accurate fitting very difficult.

2. Figures.

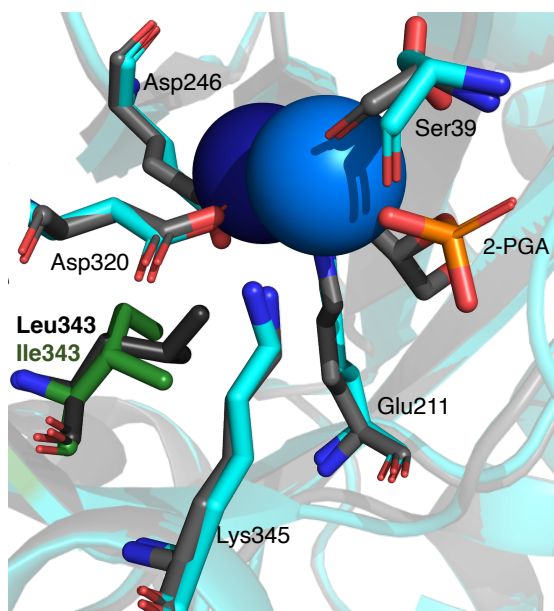


Figure S1. Modeling of Ile at position 343.

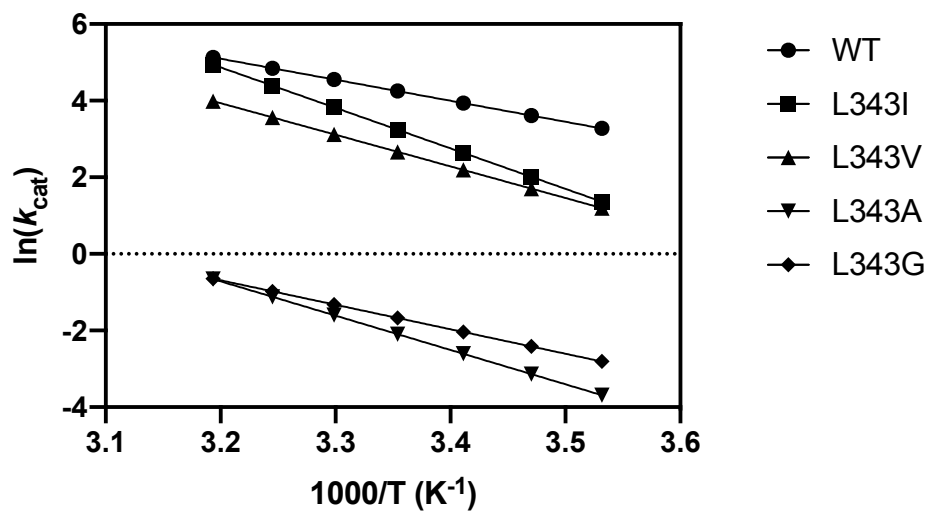


Figure S2. Activation energy of native enolase and variants studied (Leu343Ile, Leu343Val, Leu343Ala, Leu343Gly). Each point is an average of at least three experiments. Error bars are smaller than markers, and so are not visible.

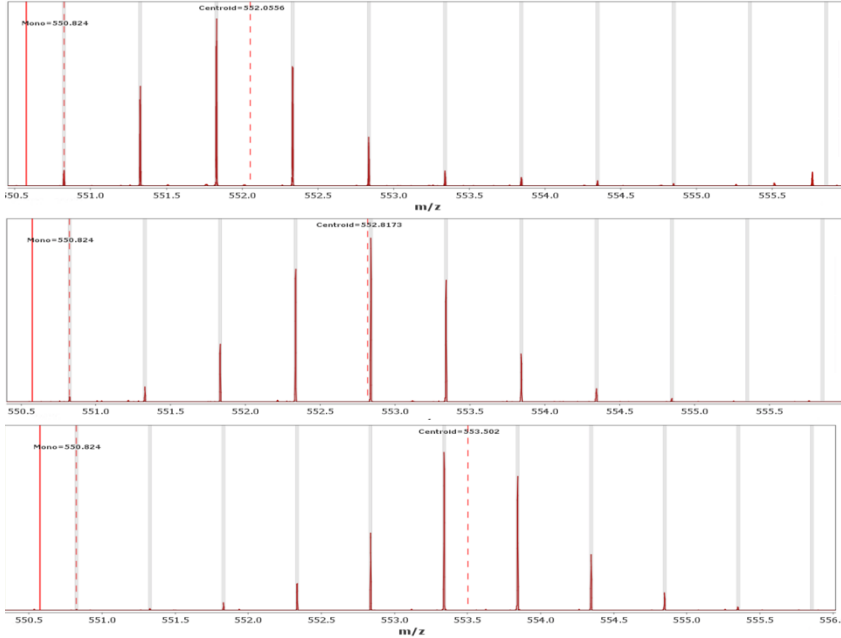


Figure S3. Example mass spectra from HDX-MS experiments showing EX2 behavior, as visualized by HDX Workbench. Data are for the $[M+2H]^{2+}$ ion of peptide 324-333 from Leu343Ala enolase.

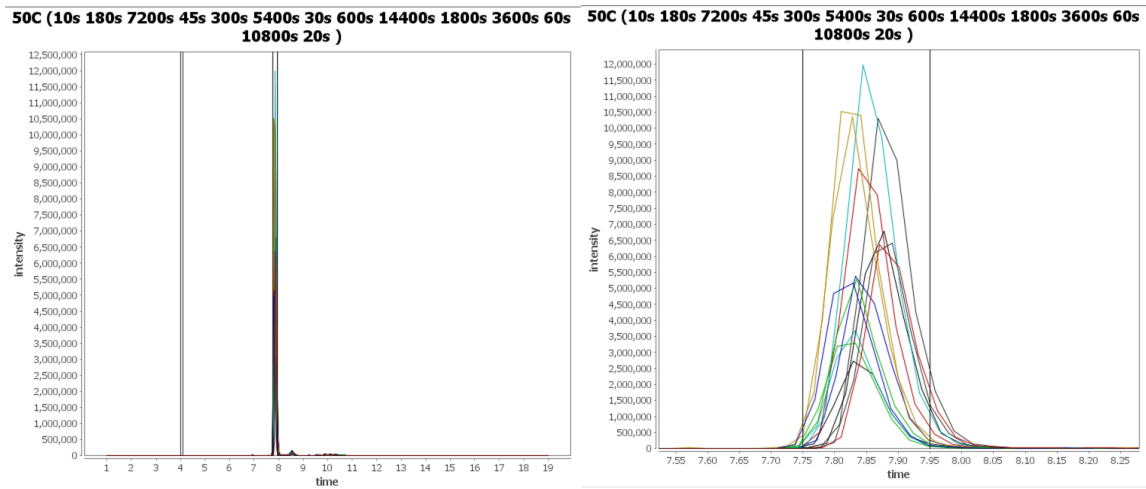


Figure S4. Consistent retention time for all time points across a day of HDX-MS experiments. Extracted ion chromatograms for Leu343Ala peptide 365-371, full retention time range (left) and zoomed in (right).

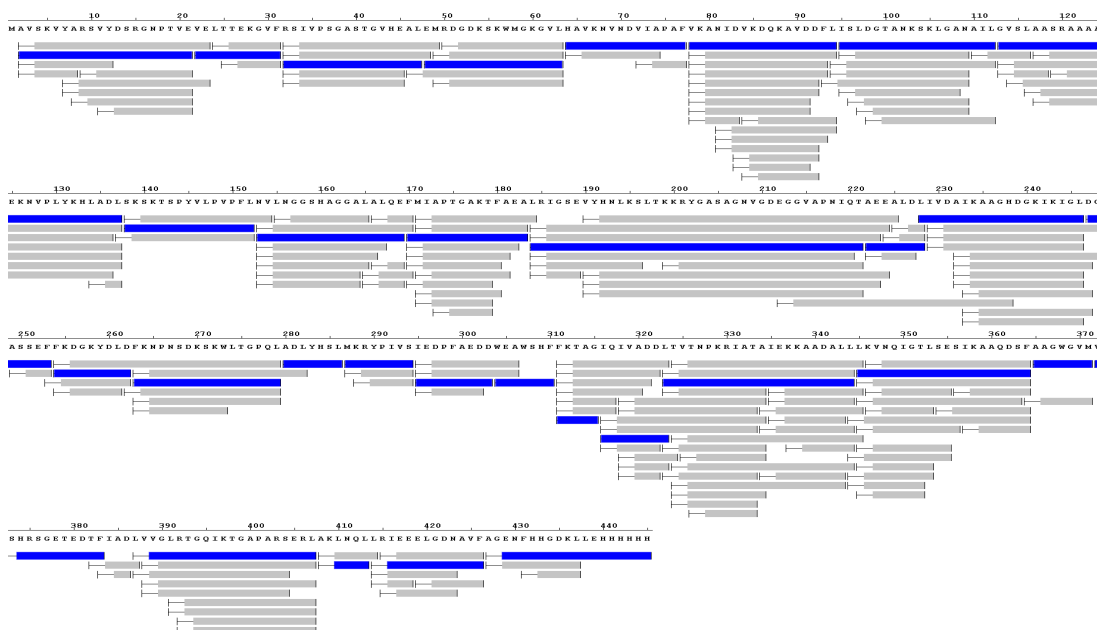


Figure S5. Sequence coverage of WT enolase by tandem mass spectrometry and tabulated using HDX Workbench.⁸ The peptides highlighted in blue indicate the selected non-overlapping peptide set.

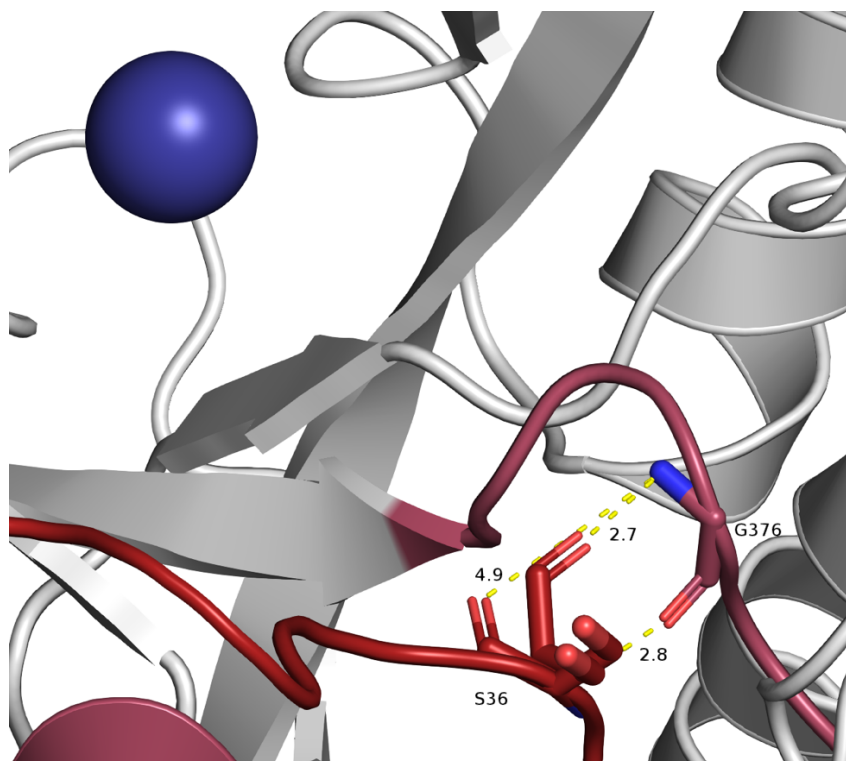


Figure S6. Hydrogen bonding interaction between Ser36 and Gly376 in Region B of the protein. Both orientations of Ser36 in the open crystal structure (PDB 1EBH) are shown. There are two H-bonds in the closer conformation and one in the farther conformation. Residues are labeled, oxygens are shown in red and nitrogens are shown in blue. Peptides are colored as in Figure 8 (peptide 32-49 in dark red, 372-383 in raspberry). Mg^{2+} is shown in dark blue.

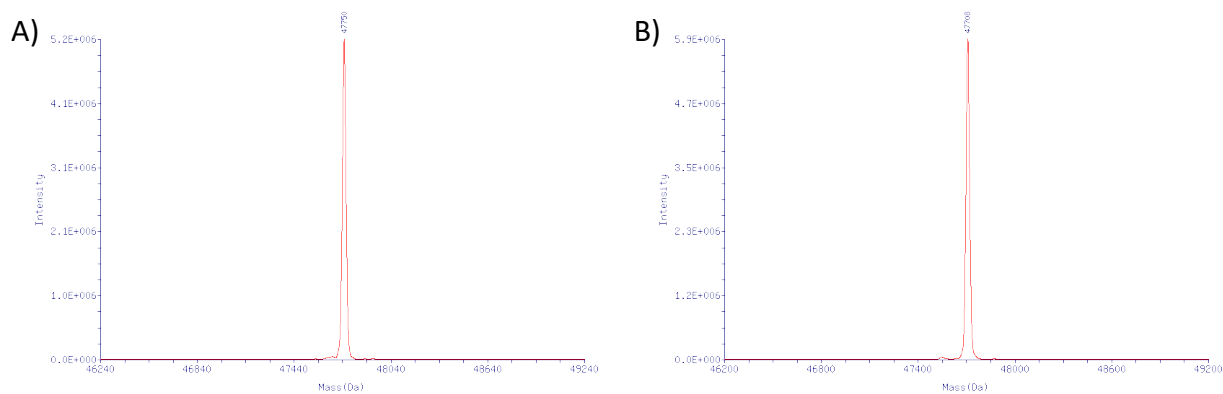


Figure S7. Intact mass spectrometry indicating purity for A) WT and B) Leu343Ala.

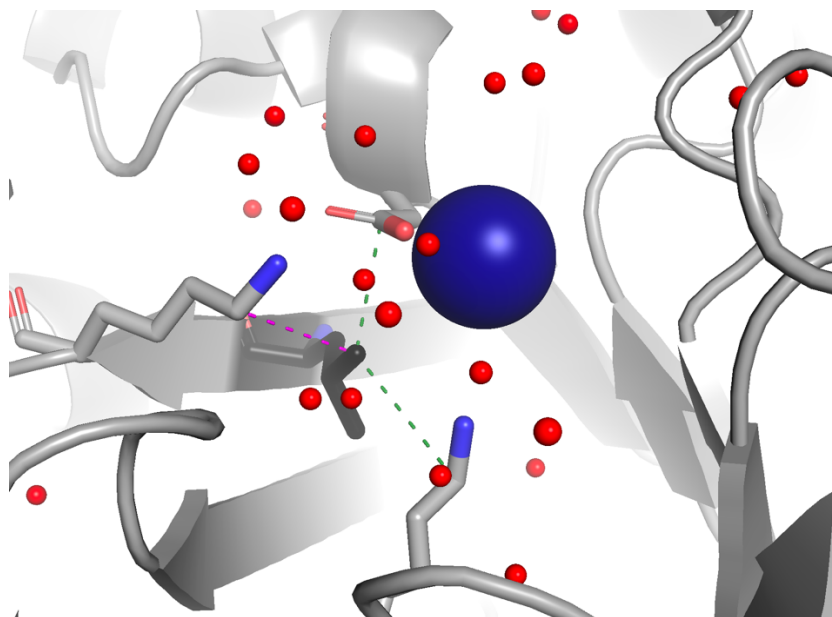


Figure S8. Structure of holo-enolase with Leu343 (black), Lys345 (left), Asp320 (center, top), and Lys396 (bottom) indicated as sticks, showing a more relaxed geometry in comparison to the structure with the substrate/product mixture. Magnesium ion is shown as a blue sphere. Water molecules are shown as red non-bonding spheres. PDB 1EBH.

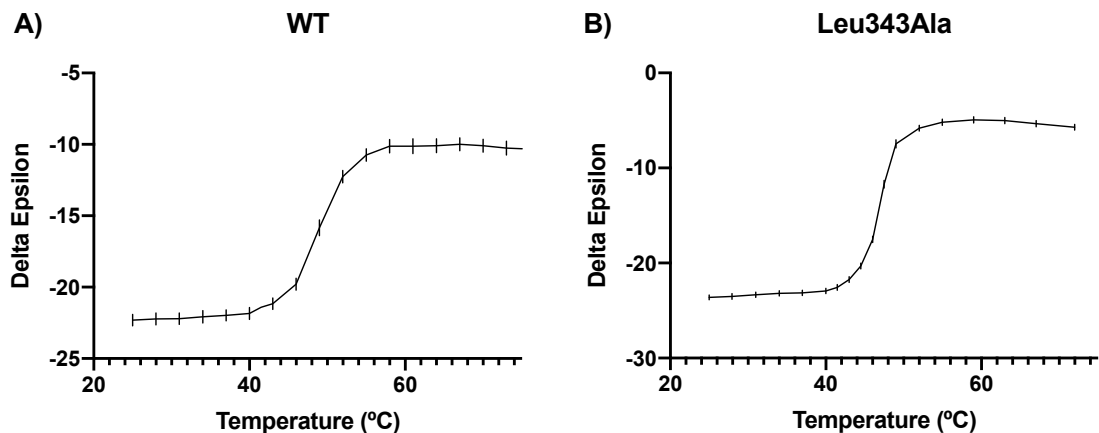


Figure S9. Circular dichroism spectra for A) WT and B) Leu343Ala at θ_{222} , with the SEM indicated by the error bars. Background corrected by subtraction of blank buffer melt.

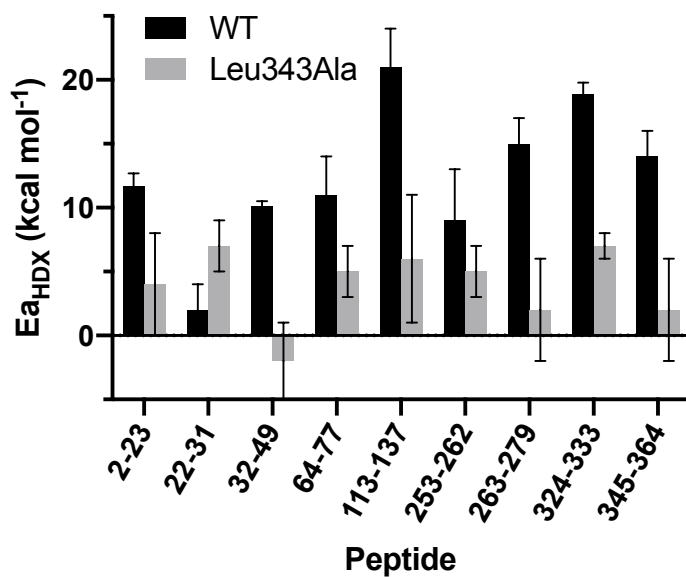


Figure S10. Graphical depiction of $E_{a_{HDX}}$ (kcal mol⁻¹) values for WT and Leu343Ala.

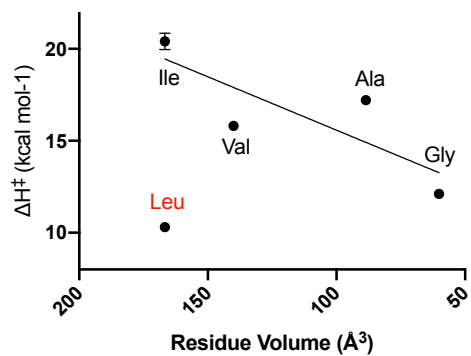


Figure S11. ΔH^\ddagger plotted as a function of the volume of the mutated residue at Leu343. The native enzyme (Leu343) is noted in red. The x-axis goes from large to small values. Error bars indicate the standard deviation, where they are not shown they are smaller than the data point.

3. Tables.

Table S1. Initial rates (s^{-1}) of enolase and variants as a function of temperature.

Temperature (°C)	WT	Leu343Ile	Leu343Val	Leu343Ala	Leu343Gly
10	27 (2)	3.9 (0.3)	3.3 (0.1)	0.025 (0.001)	0.060 (0.001)
15	36 (2)	7.5 (0.6)	5.5 (0.1)	0.043 (0.002)	0.089 (0.002)
20	52 (5)	14 (1)	9.0 (0.2)	0.074 (0.003)	0.130 (0.003)
25	74 (2)	26 (2)	14.4 (0.3)	0.123 (0.005)	0.188 (0.004)
30	104 (3)	46 (4)	22.7 (0.5)	0.20 (0.01)	0.27 (0.01)
35	126 (10)	81 (6)	35.3 (0.7)	0.33 (0.01)	0.38 (0.01)
40	165 (17)	140 (11)	54 (1)	0.52 (0.02)	0.52 (0.01)

All experiments were carried out in 50 mM HEPES, 2 mM $MgCl_2$ at pH 7.5, and the number in parentheses is the standard deviation.

Table S2. Non-overlapping peptide set with back exchange values. The mutation site (L343) is marked in red. Back exchange values were the same for both WT and Leu343Ala.

Sequence	Start	End	Charge	Back Exchange (%)
AVSKVYARSVYDSRGNPTVEVE	2	23	3	60.73
VELTTEKGVF	22	31	2	35.56
RSIVPSGASTGVHEALEM	32	49	2	44.66
EMRDGDKSKWMGKGVL	48	63	3	52.95
HAVKNVNDVIAPAF	64	77	2	31.41
VKANIDVKDQKAVDDFL	78	94	3	51.16
LISLDGTANKSKLGANAIL	94	112	2	43.90
GVSLAASRAAAAEKNVPLYKHLADL	113	137	4	43.64
SKSKTSPYVLPVPFL	138	152	2	36.03
NVLNGGSHAGGALALQEF	153	170	2	48.28
FMIAPTGAKTFAEA	170	183	2	41.89
LRIGSEVYHNLKSLTKKRYGASAGNVGDEGGVA PNIQTAE	184	223	5	40.77
EALDL	224	228	1	36.87
IVDAIKAAGHDGKIKIGLDCASSEF	229	253	3	38.55
FFKDGKYDLD	253	262	2	56.35
FKNPNSDKSKWLTGPQL	263	279	2	50.87
ADLYHSL	280	286	2	45.06
MKRYPIVS	287	294	2	21.84
IEDPFAEDD	295	303	1	47.84
WEAWSHF	304	310	2	55.79

FKTAGIQIVADDL	311	323	2	20.00
TVTNPKRIAT	324	333	2	16.60
AIEKKAADALL	334	344	2	30.32
LKVNQIGTLSESIKAAQDSF	345	364	3	24.89
AAGWGVM	365	371	1	21.25
VSHRSGETEDTF	372	383	2	62.78
FIAD	383	386	1	26.51
LVVGLRTGQIKTGAPARSERL	387	407	4	38.97
AKLNQL	408	413	1	19.86
LRIIEELGDNAVF	414	426	2	63.27
AGENFHGDKLLEHHHHHH	427	445	4	59.71

Table S3: HDX-MS classification of enolase, based on the classification system used for COMT and mADA.^{9,13}

Class	# Amides	% Enolase	Peptides
Type I: Rapid exchange, at the upper limit of k_{fast} – appear temperature independent	26	6	224-228, 383-386, 408-413, 427-445
Type II A: Peptides with highly temperature-dependent exchange and reach a plateau	233	52	2-23, 22-31, 32-49, 48-63, 64-77, 263-279, 280-286, 287-294, 304-310, 311-323, 324-333, 414-426
Type II B: Peptides that do not reach an apparent plateau at long times and high temperature	131	29	78-94, 94-112, 113-137, 138-152, 153-170, 170-183, 184-223, 229-253, 253-262, 295-303, 334-344, 345-364, 365-371, 372-383, 387-407

Table S4. Regions that undergo shifts greater than 3 Å in the crystal structure upon substrate/product binding. Crystal structure PDB identifiers 1EBH and 1ONE.

Loop #	Residues	Location & Key Residues	Shift Range (Å)
1	37 - 42	Mg ²⁺ binding loop (Ser39)	3.9 – 11.6
2	156 - 165	Loop between TIM barrel sheets 1 and 2; substrate binding loop (His159)	3.3 – 6.5
3	252 - 276	Loop between TIM barrel sheet 3 and helix 6	3.0 – 6.1

Table S5. HDX data summary for WT and Leu343Ala.

Data sets	WT & Leu343Ala
HDX Reaction Details	Labeling conditions: 10 μM protein, 90% D ₂ O, 10 mM HEPES, 2 mM MgCl ₂ , pH _{read} = 7.1. 0s time point was collected with 10μM protein, 100% H ₂ O, 10 mM HEPES, 2 mM MgCl ₂ , pH = 7.5. HDX was conducted at five different temperatures: 10, 20, 25, 30, 40 °C
HDX Time Course	0, 10, 20, 30, 45, 60, 180, 300, 600, 1800, 3600, 5400, 7200, 10800, 14400 seconds
HDX Controls	Maximally labeled control (WT and Leu343Ala)

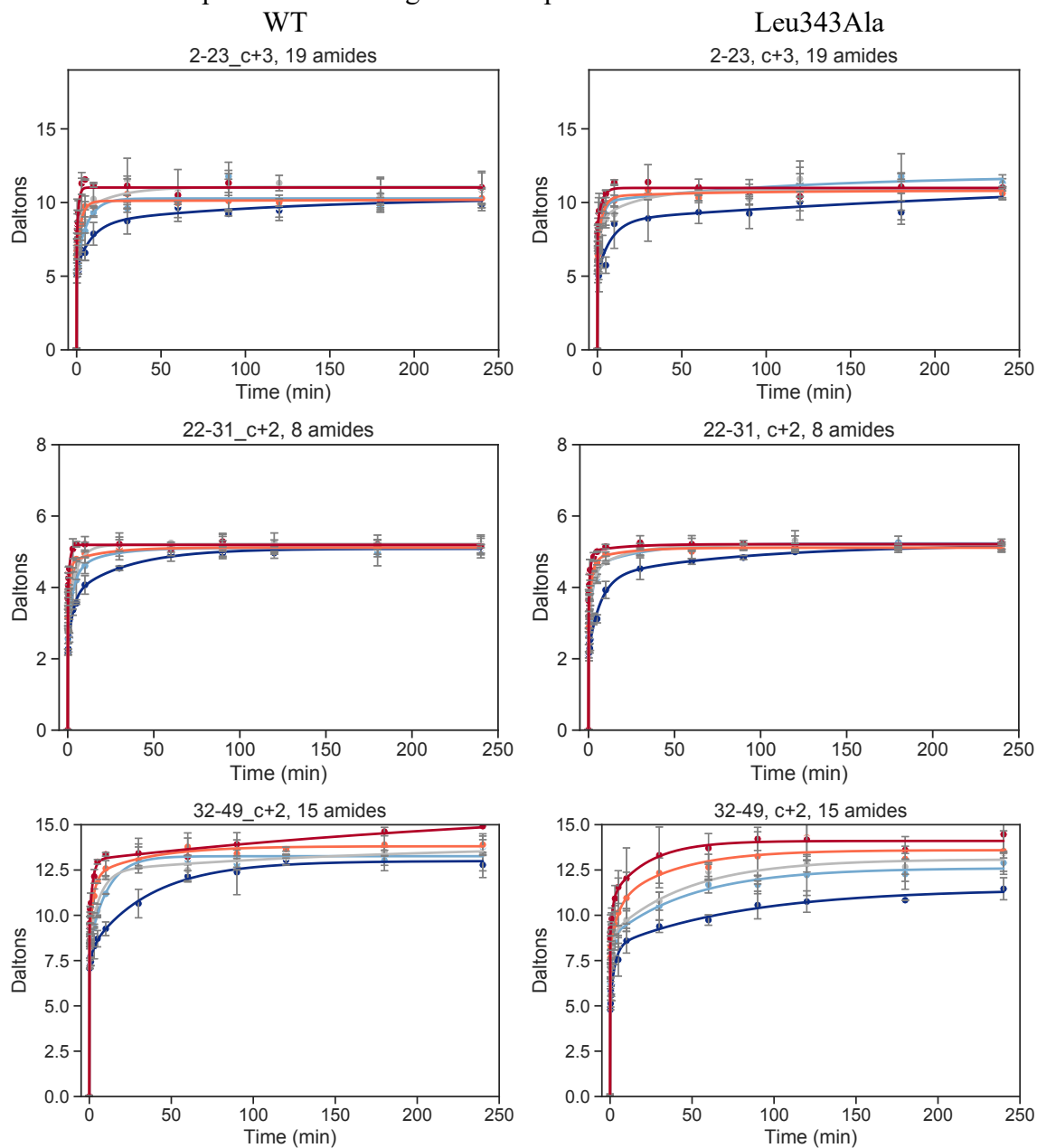
	Possible peptides from the protease used for digestion were searched for in all data sets. MS was validated in an earlier study. ¹⁰
Back Exchange: Average, Interquartile	40.9%, 20.1%
Number of Peptides	31 chosen for analysis (see Table S2)
Sequence Coverage	84.5% of amides were measurable
Average Peptide Length	12.6 amides
Replicates	2 (biological) Each time point for each temperature for each protein was collected twice, with each replicate coming from a different protein expression. Due to the scale of the experiment, it was impractical to collect a third replicate at all points. To mitigate systematic errors, each temperature set (15 time points of one protein) was collected over three days in a non-sequential order.
Repeatability	The average standard deviation for all WT data points across all temperatures is 0.27 amides.
Significant Differences in HDX	In this study we used $\Delta E_{a\text{HDX}}$ to quantify the differences between data sets. Values that were larger than their error were considered a significant difference between protein states.

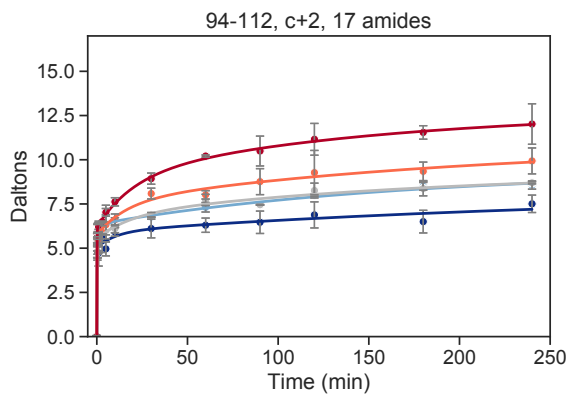
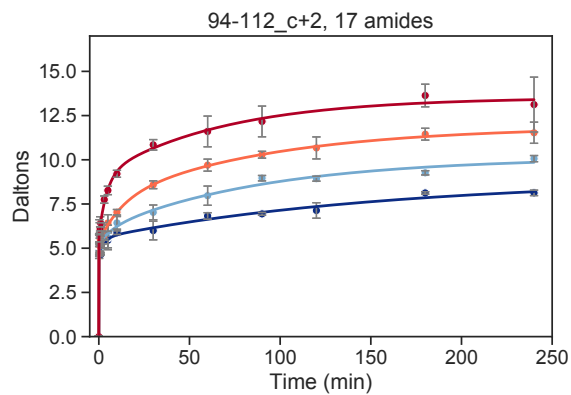
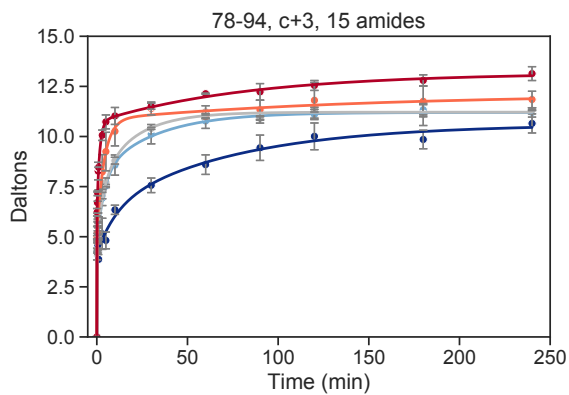
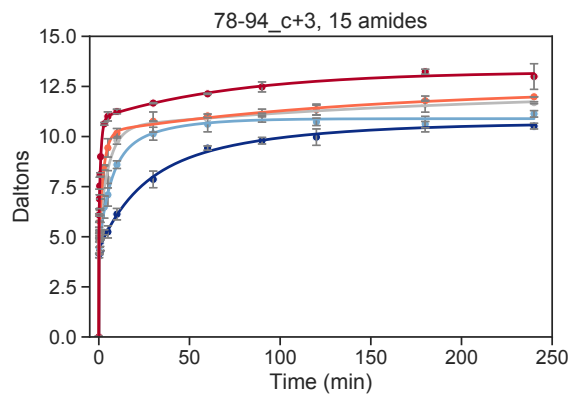
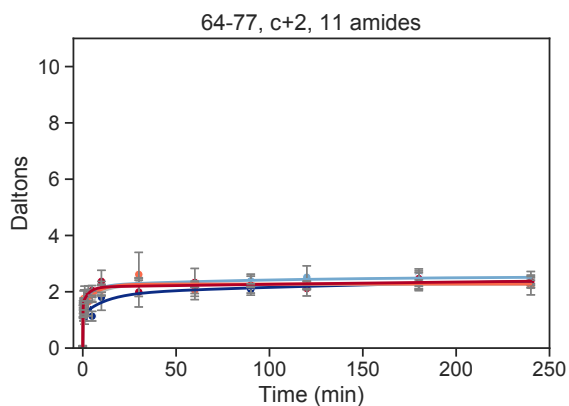
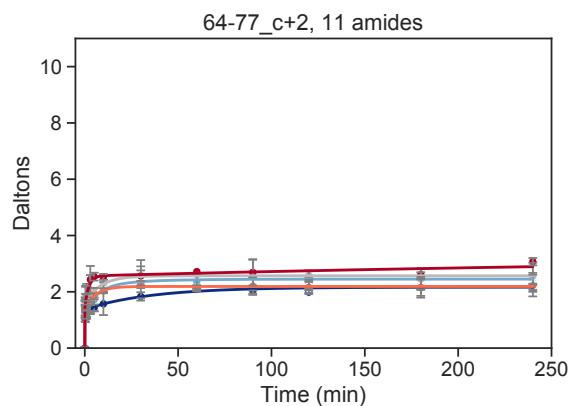
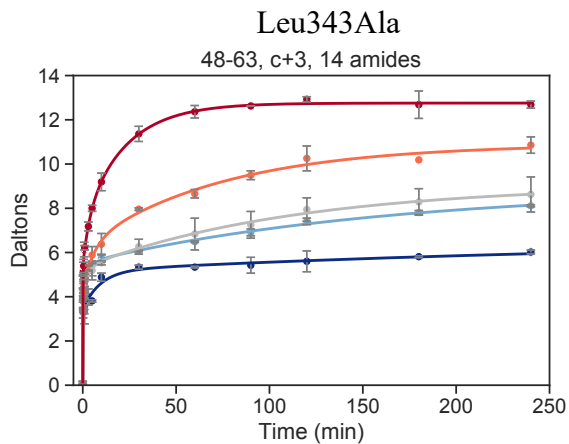
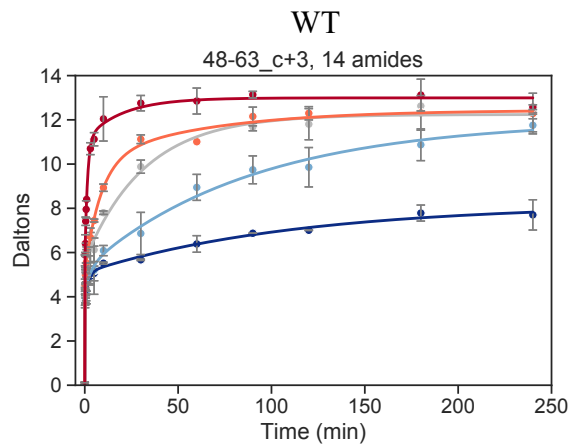
Table S6. $E_a(\text{HDX})$ values for all Type II peptides. The notes column indicate those peptides included in Table 2 (where $\Delta E_a(\text{HDX}) > \text{error}$). Exceptions, also noted, are discussed in section SI 1.p. $\Delta E_a(\text{HDX}) = E_a(\text{HDX})(\text{Leu343Ala}) - E_a(\text{HDX})(\text{WT})$.

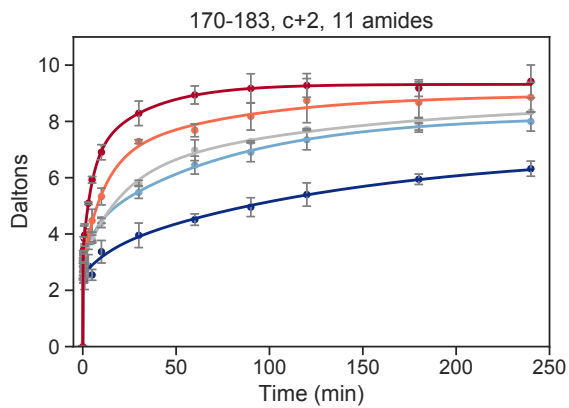
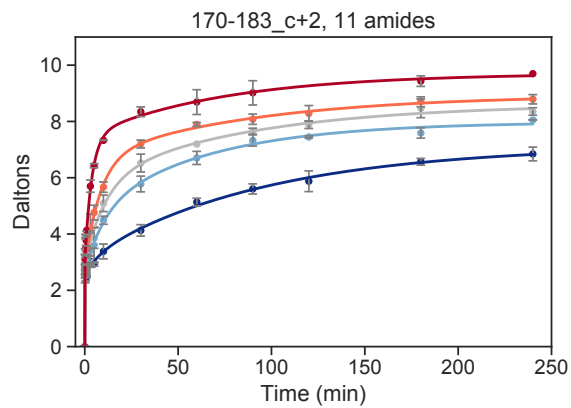
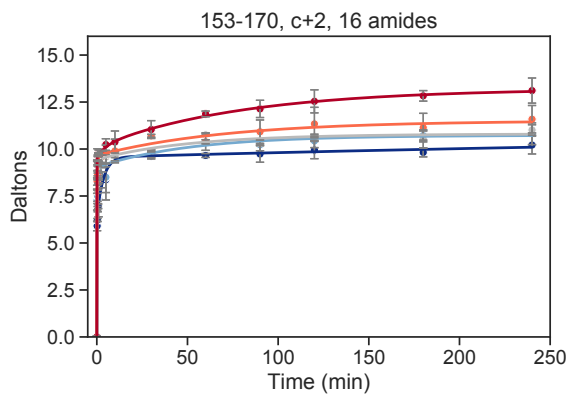
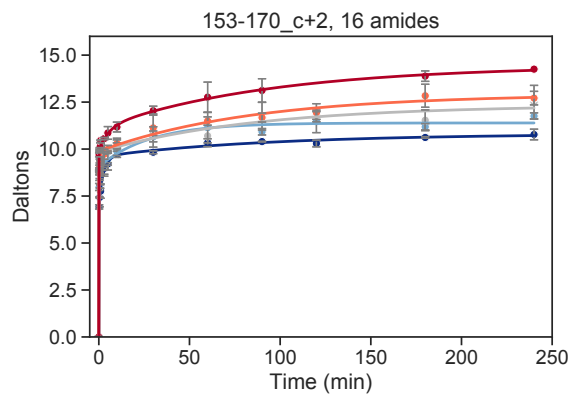
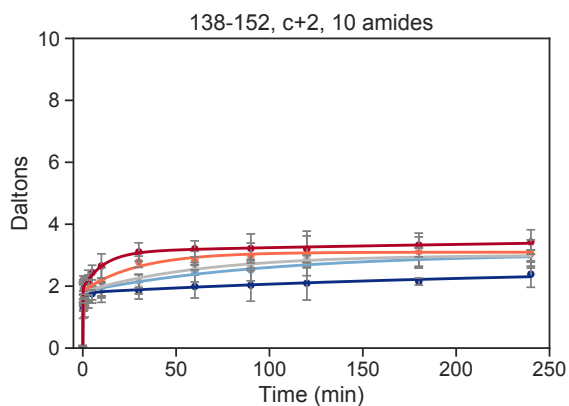
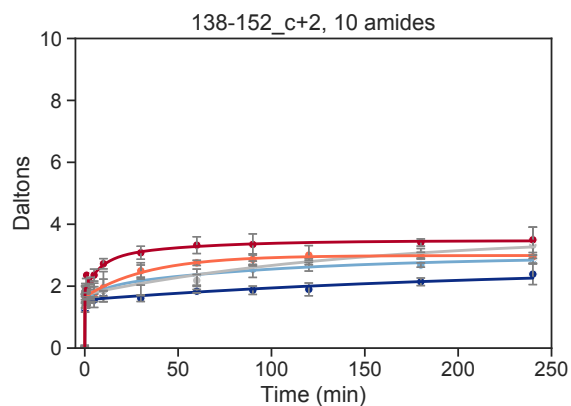
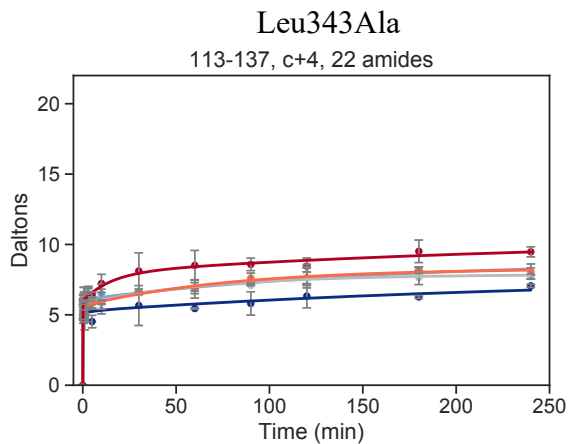
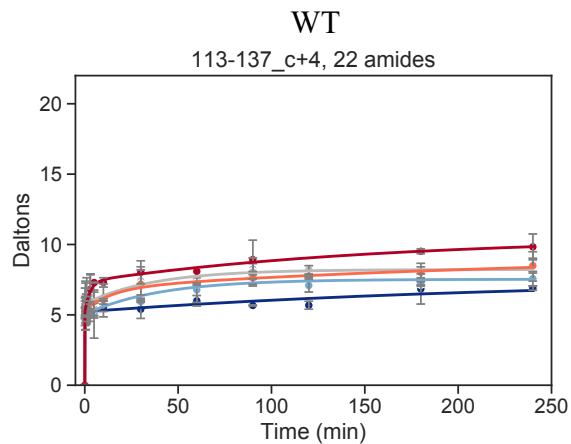
Peptide	WT $E_a(\text{HDX})$	L343A $E_a(\text{HDX})$	$\Delta E_a(\text{HDX})$	Notes
113-137	21 (3)	6 (5)	-15 (6)	in Table 2
263-279	15 (2)	2 (4)	-12 (4)	in Table 2
345-364	14 (2)	2 (4)	-12 (5)	in Table 2
324-333	18.9 (0.9)	7 (1)	-12 (2)	in Table 2
32-49	10.1 (0.4)	1 (4)	-9 (4)	in Table 2
2-23	12 (1)	4 (4)	-8 (4)	in Table 2
64-77	11 (3)	5 (3)	-6 (4)	in Table 2
372-383	13.1 (0.8)	11 (1)	-2 (1)	in Table 2
22-31	2 (2)	7 (2)	5 (3)	in Table 2
78-94	16 (1)	16 (2)	-1 (2)	
170-183	15.2 (0.9)	13 (3)	-3 (3)	
311-323	7 (3)	5 (2)	-1 (3)	
229-253	8 (3)	5 (2)	-3 (4)	
365-371	9 (4)	10 (3)	1 (5)	
304-310	15 (3)	11 (4)	-3 (5)	
334-344	19 (3)	21 (4)	2 (5)	
48-63	11 (6)	7 (2)	-4 (6)	
253-262	9 (4)	5 (2)	-4 (4)	
153-170	8 (5)	13 (6)	5 (8)	

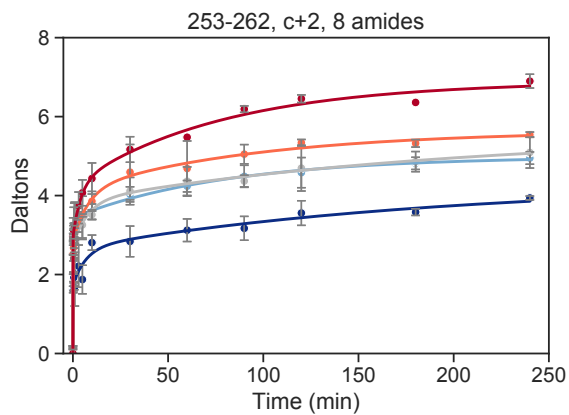
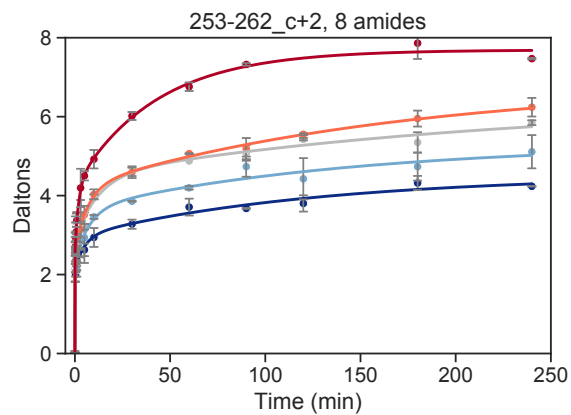
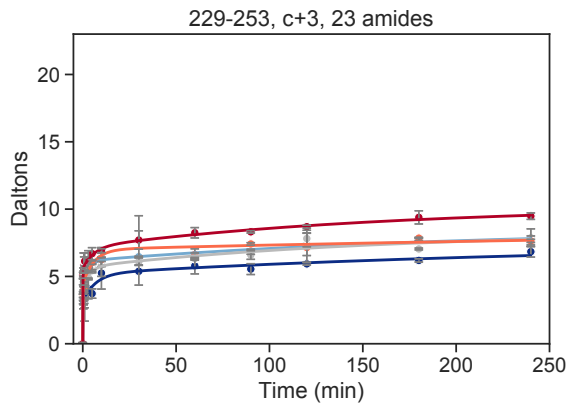
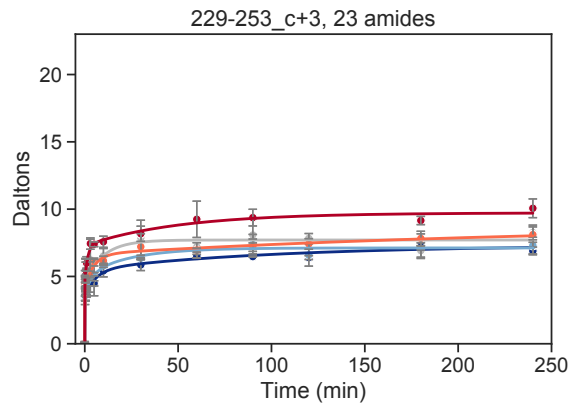
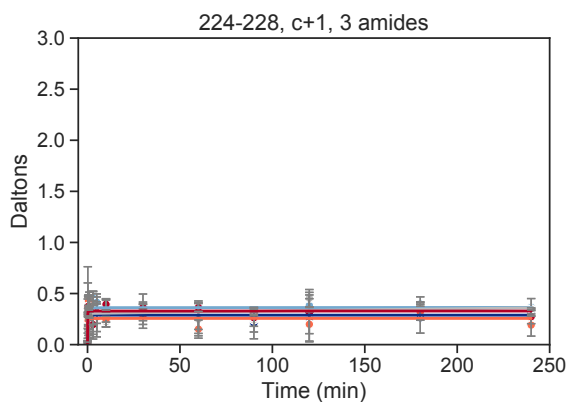
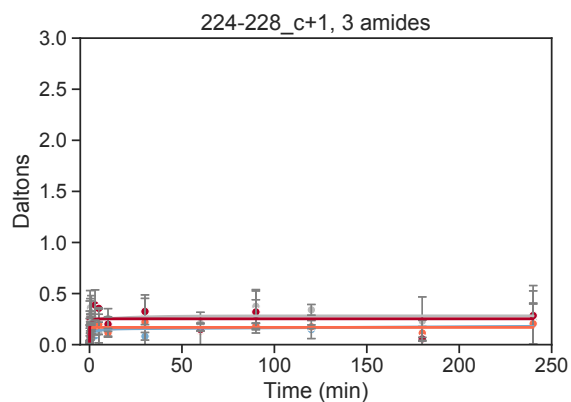
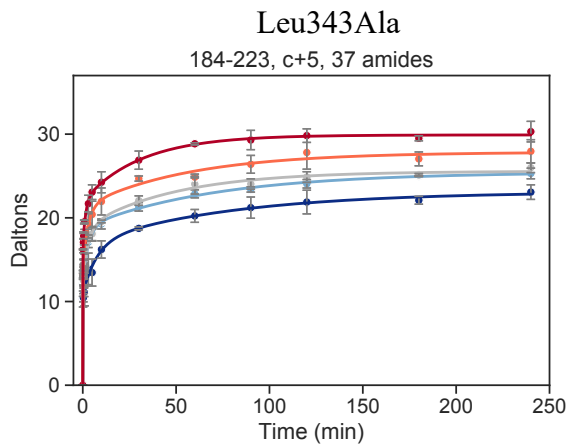
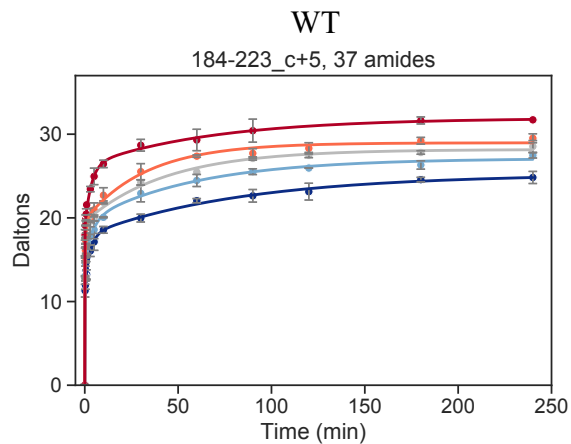
184-223	10 (8)	8 (2)	-2 (8)	
94-112	3 (6)	1 (6)	-2 (9)	
295-303	13 (3)	2 (12)	-11 (12)	
414-426	9 (5)	6 (3)	-2 (5)	
287-294	-2 (10)	-24 (12)	-22 (16)	Discussed in SI 1.p
280-286	21 (5)	-9 (10)	-30 (11)	Discussed in SI 1.p
387-407	27 (11)	3 (8)	-24 (13)	Discussed in SI 1.p
138-152	11 (6)	20(2)	8 (6)	Discussed in SI 1.p

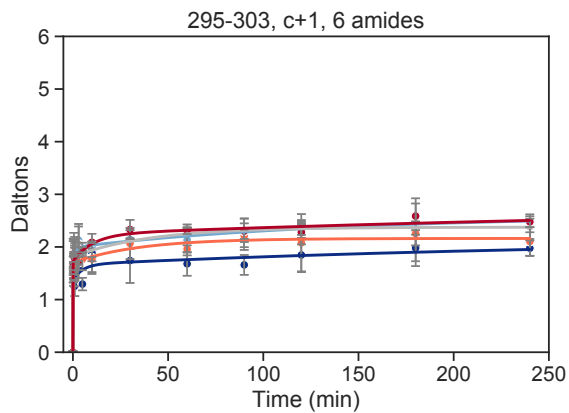
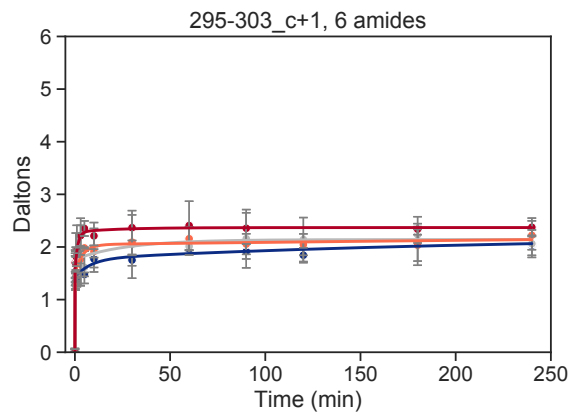
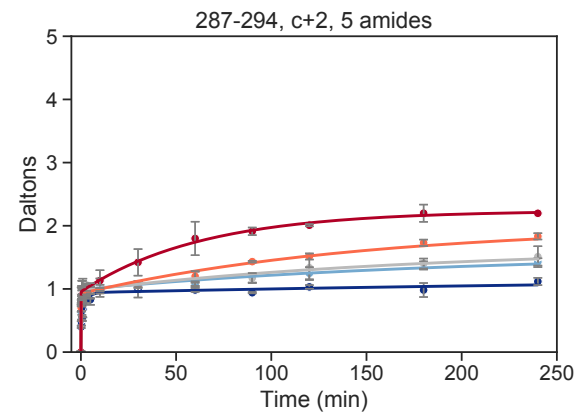
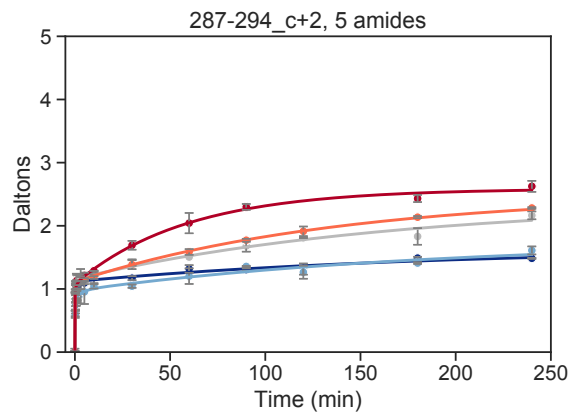
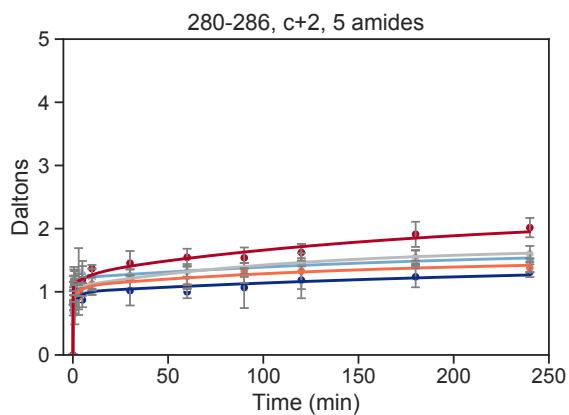
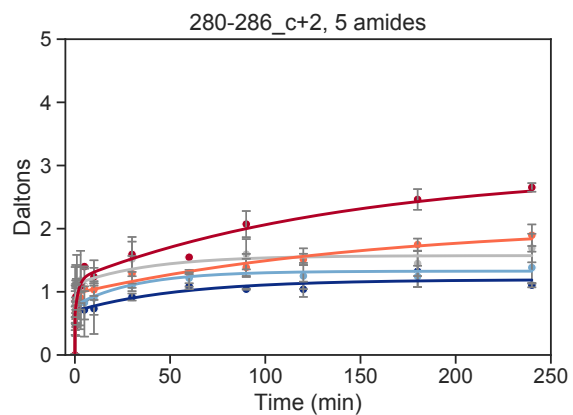
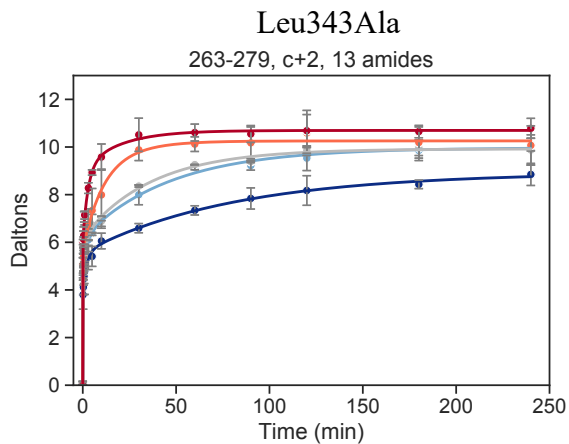
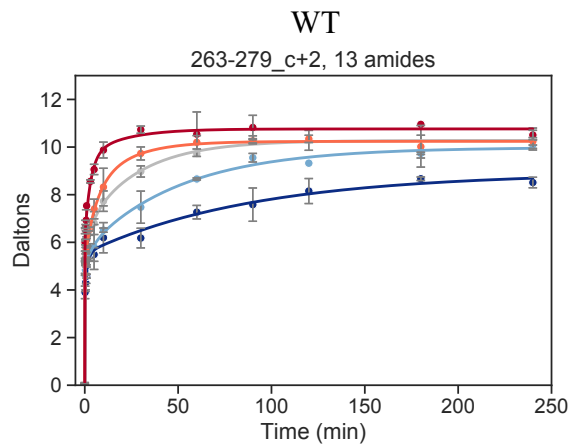
4. **HDX Uptake Plots.** HDX-MS deuterium uptake plots for all peptides. Each peptide has been corrected for back exchange individually. WT peptides are in the left column and Leu343Ala peptides are shown in the right column. HDX is plotted as Daltons versus minutes, and the different temperatures are indicated by colored lines and points (40 °C - red, 30 °C - orange, 25 °C - grey, 20 °C - light blue, and 10 °C - dark blue). Error bars indicate the standard deviation for each data point as the average of two replicates.

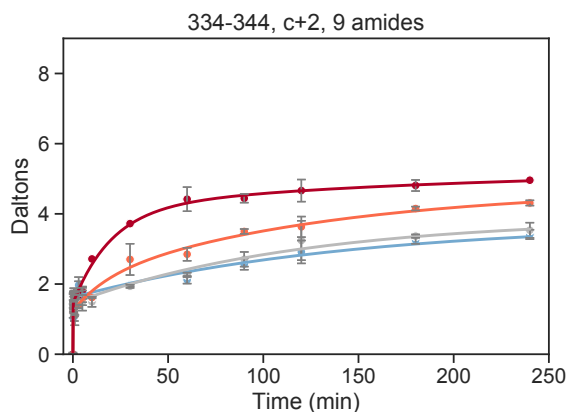
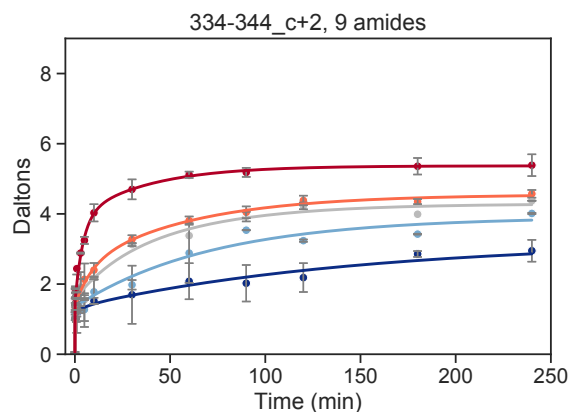
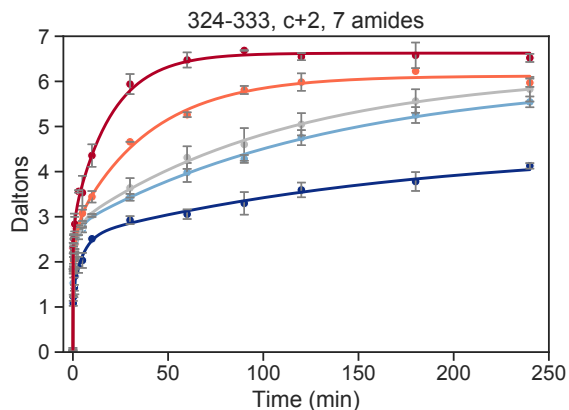
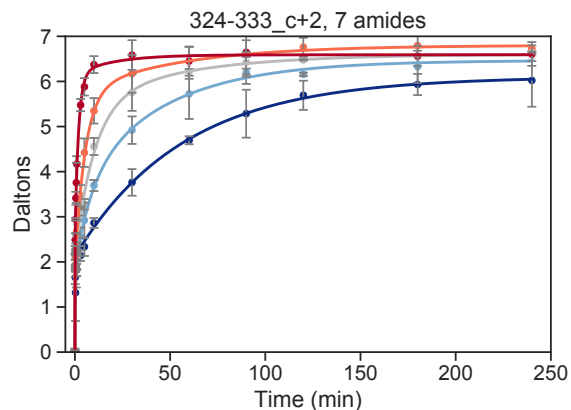
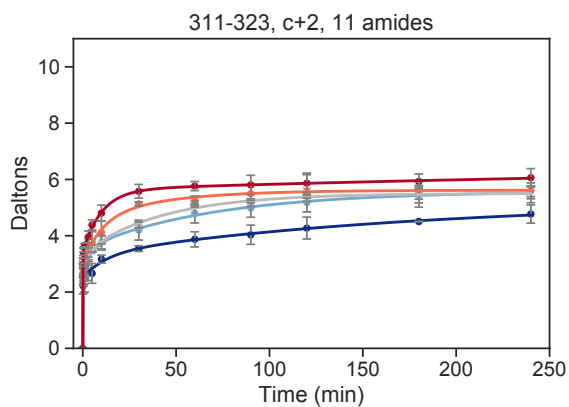
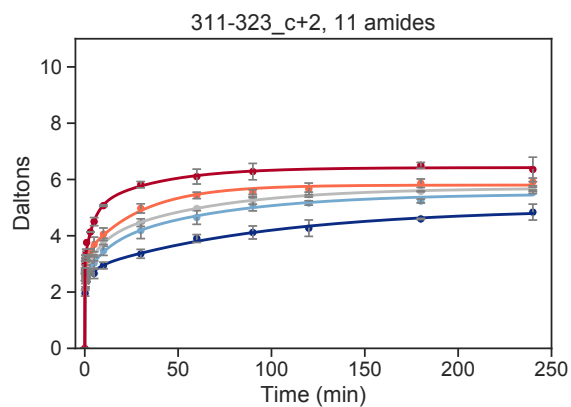
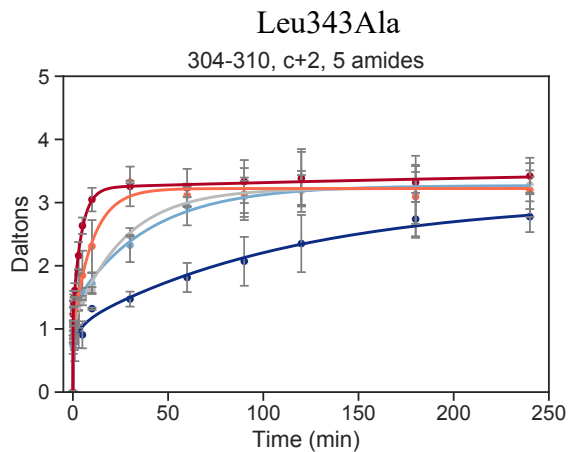
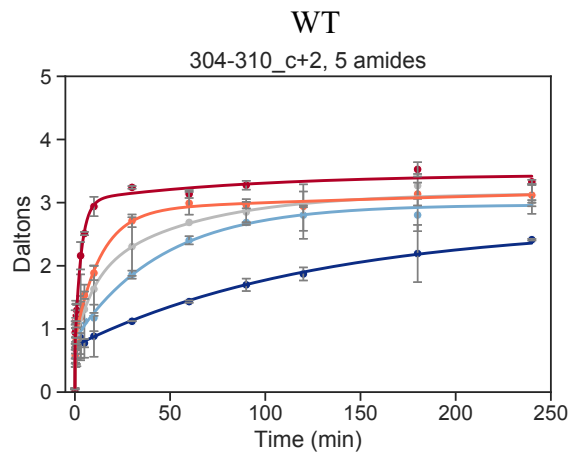


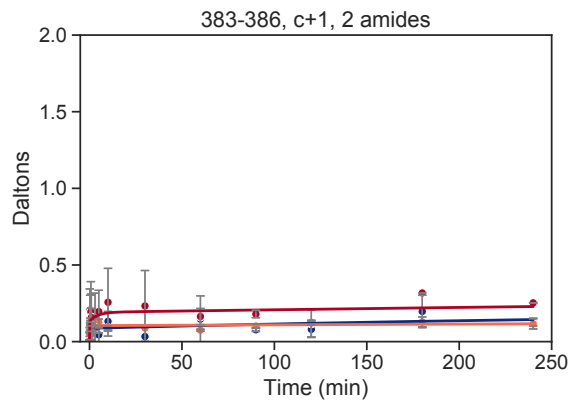
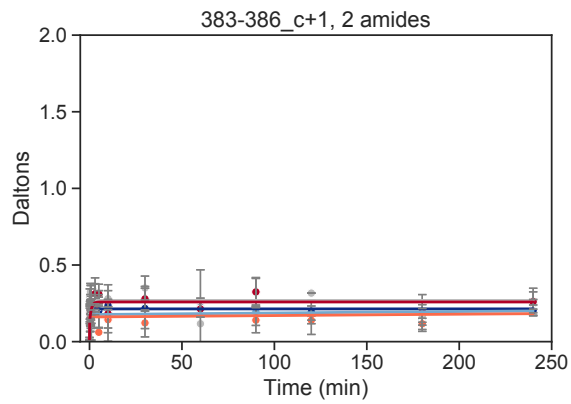
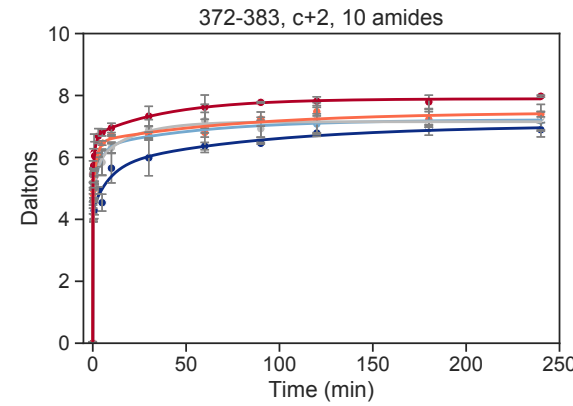
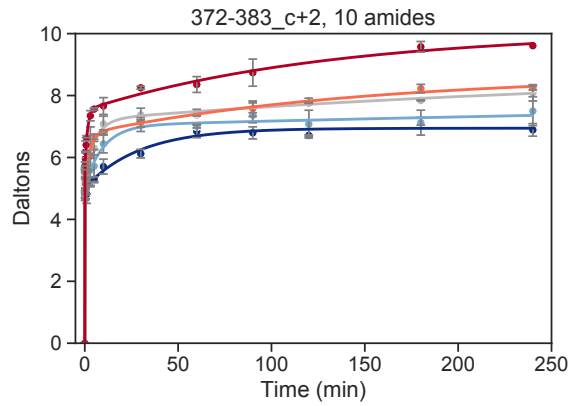
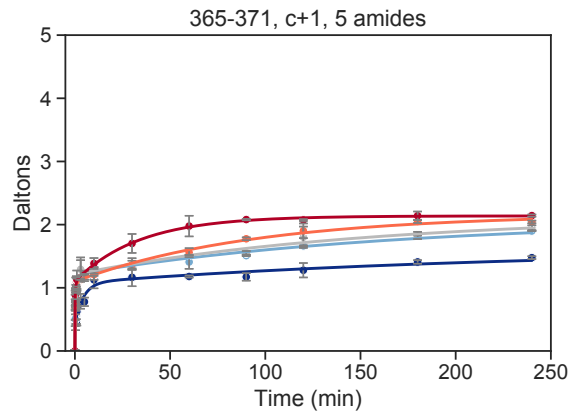
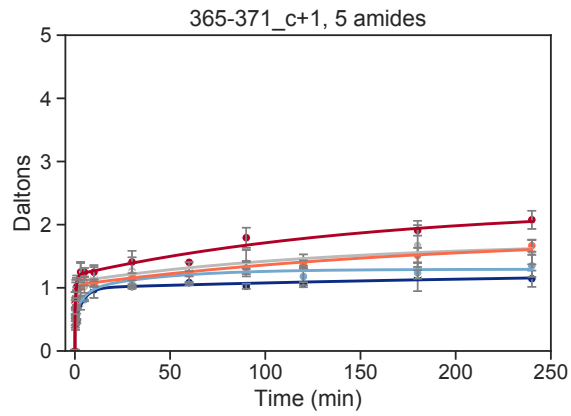
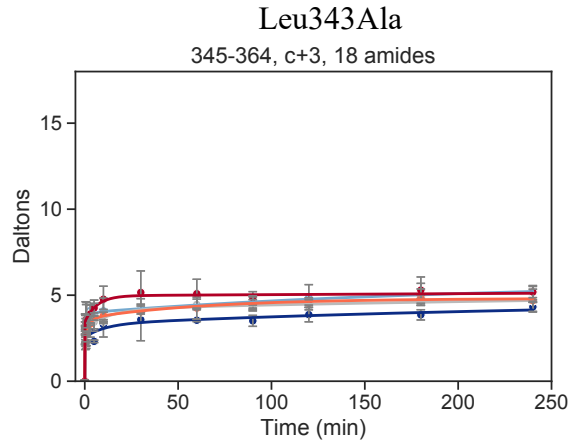
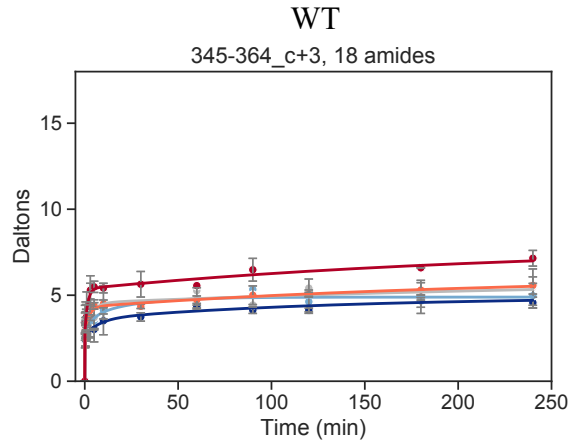


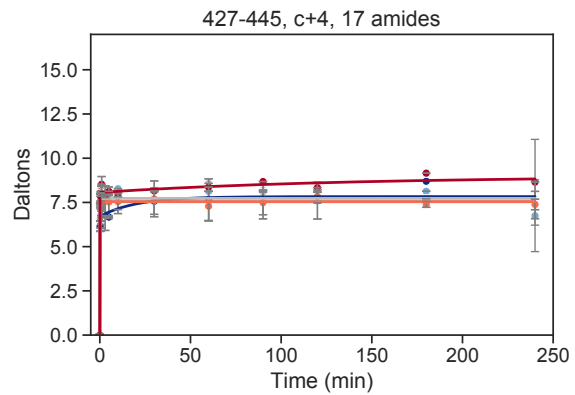
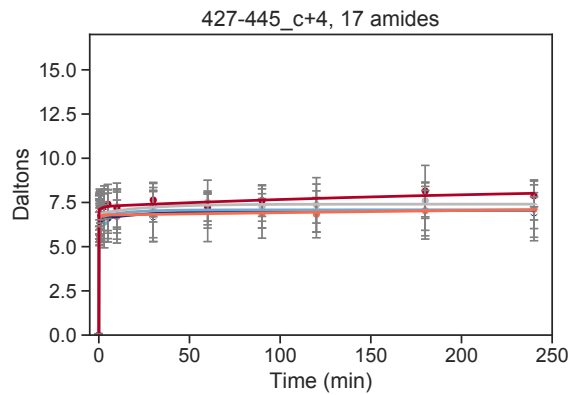
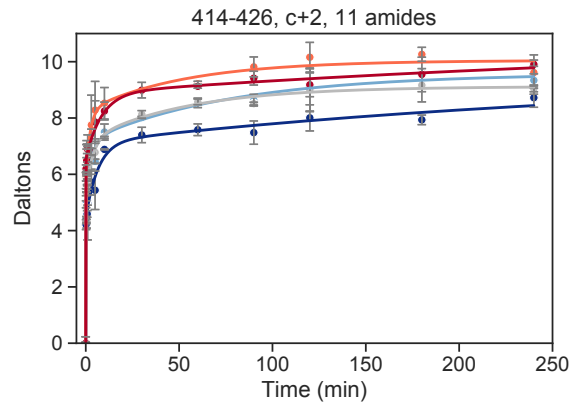
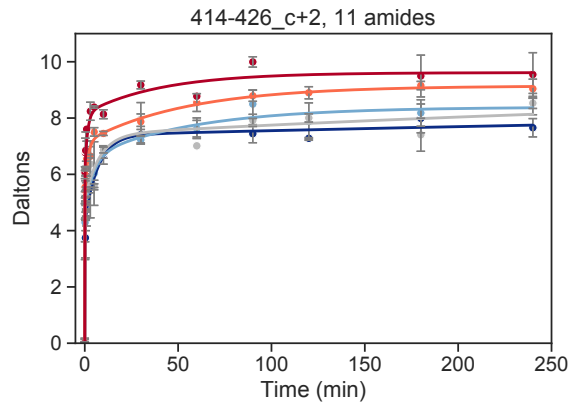
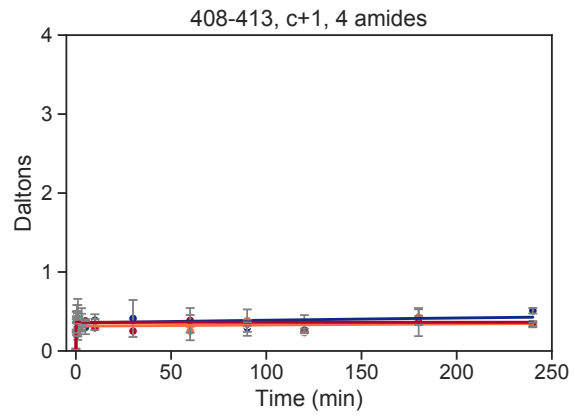
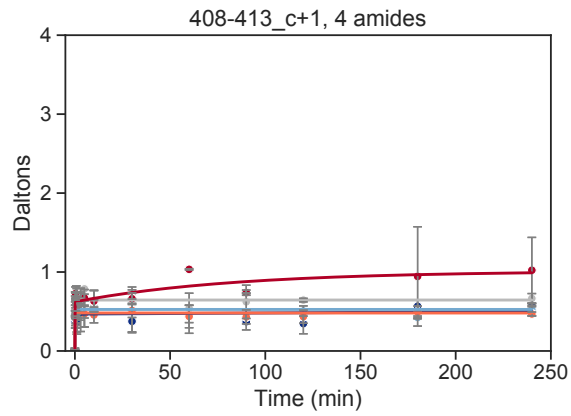
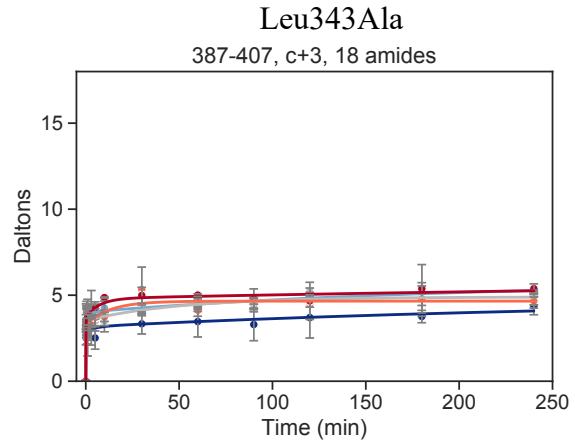
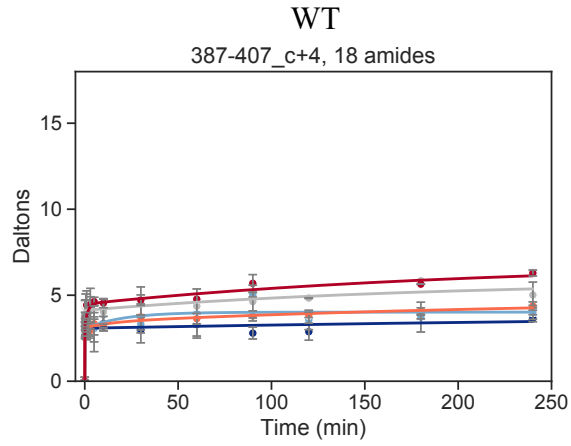




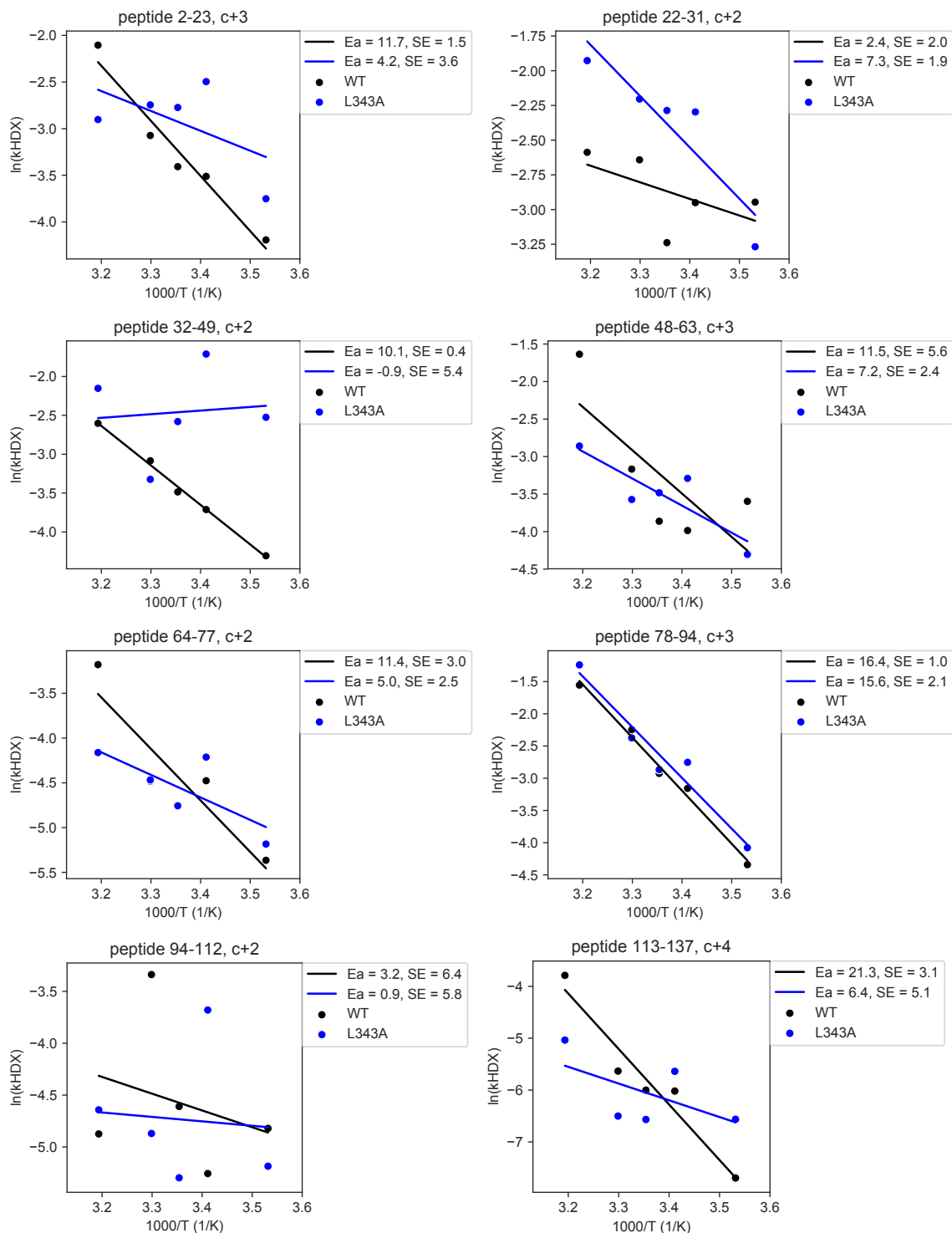


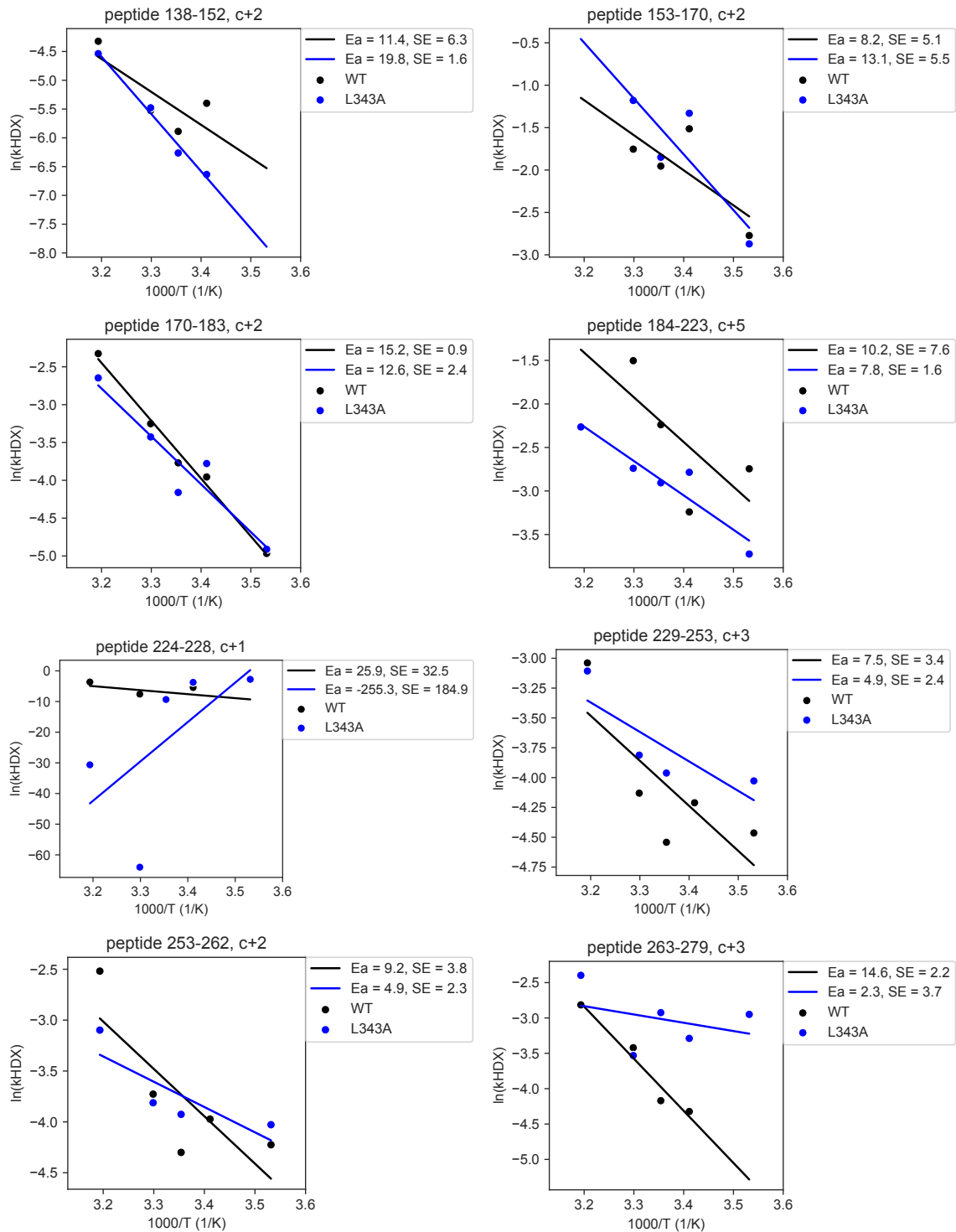


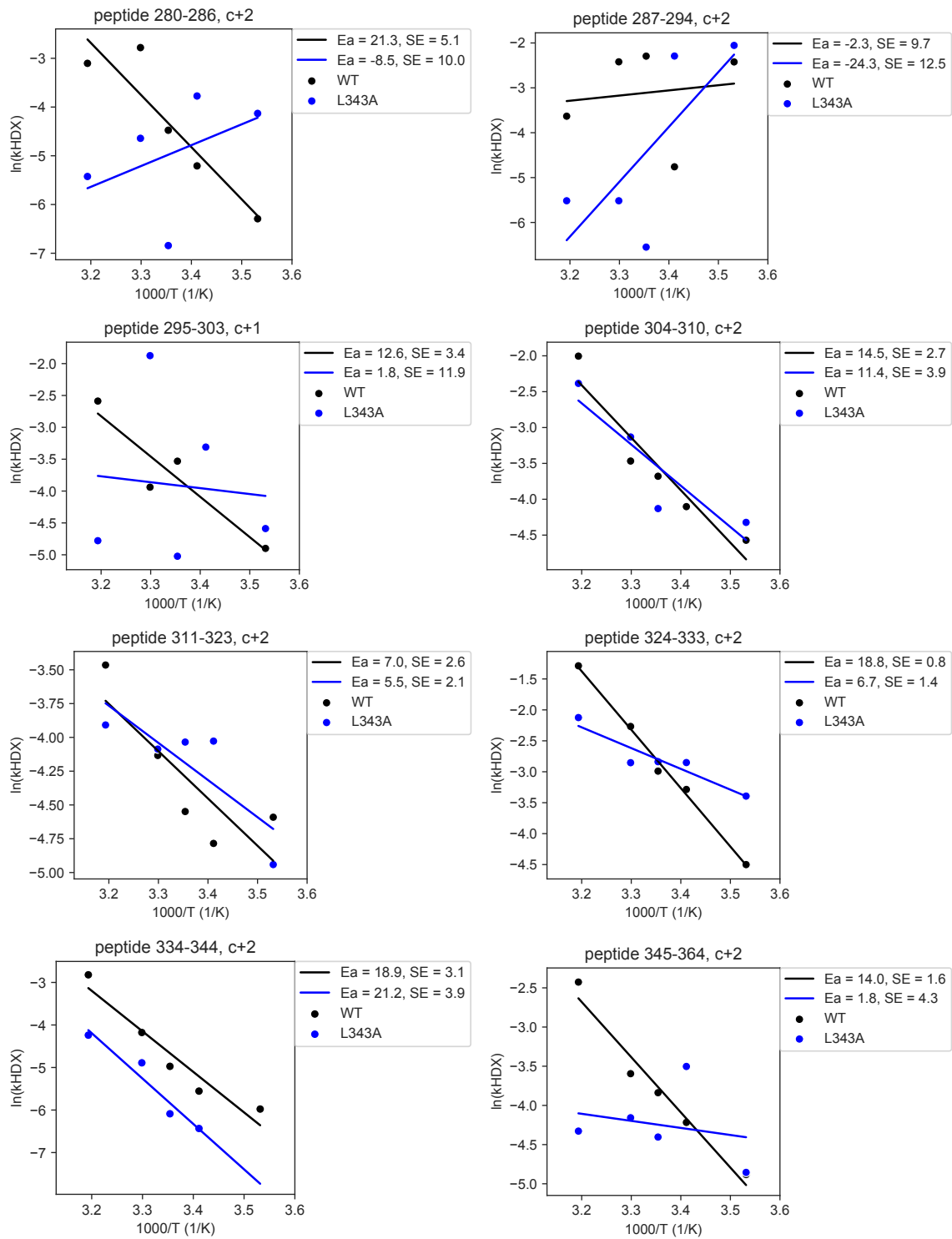


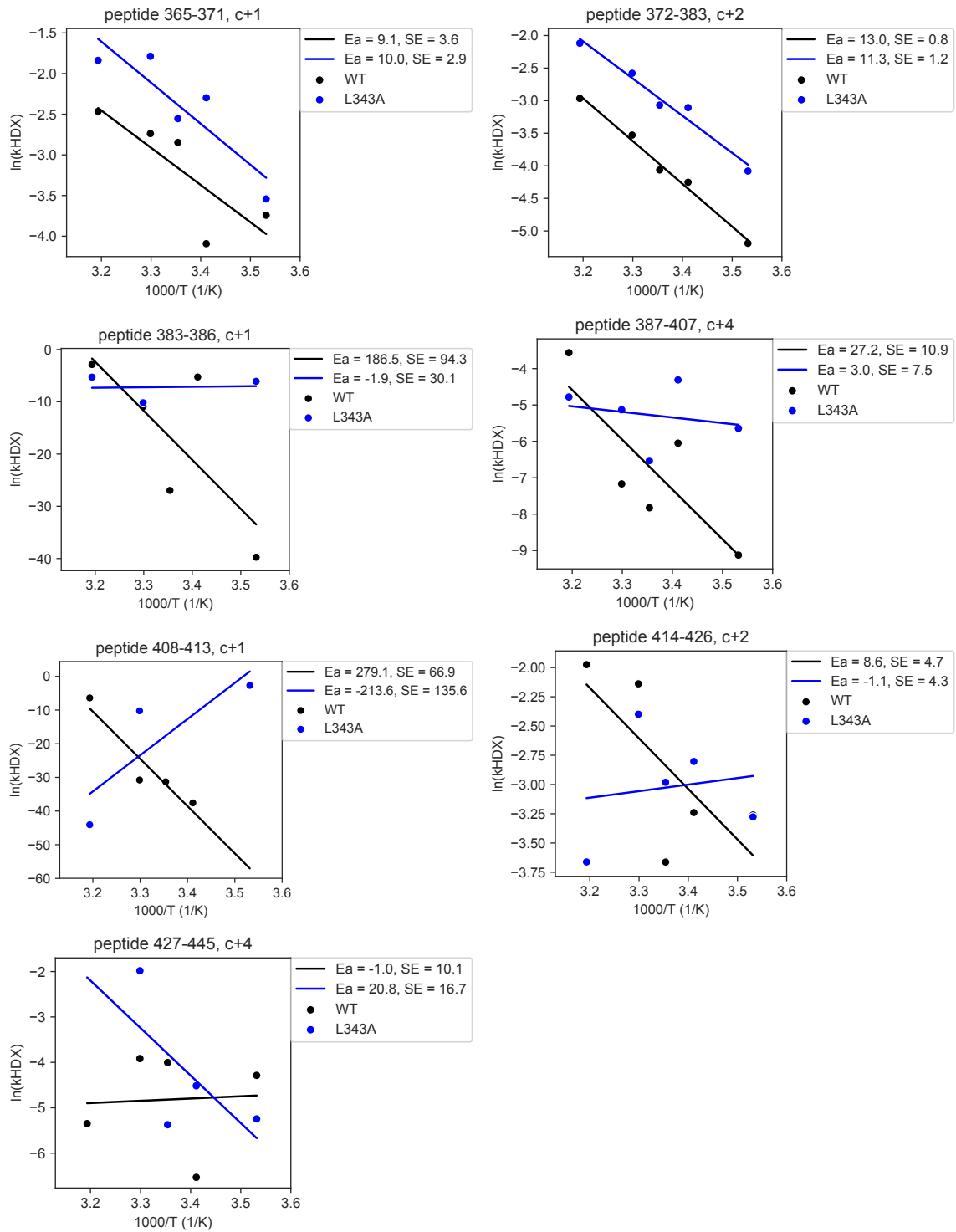


5. **E_{aHDX} Plots.** HDX-MS deuterium uptake plots for all peptides. Each peptide has been corrected for back exchange individually. WT peptides are in the left column and Leu343Ala peptides are shown in the right column. HDX is plotted as Daltons versus minutes, and the different temperatures are indicated by colored lines and points (40°C - red, 30°C - orange, 25°C - grey, 20°C - light blue, and 10°C - dark blue).









6. References.

1. Sims, P. A.; Reed, G. H. Method for the Enzymatic Synthesis of 2-Phospho-D-Glycerate From Adenosine 5'-Triphosphate and D-Glycerate via D-Glycerate-2-Kinase. *J. Mol. Cat. B: Enzym.* **2005**, *32* (3), 77–81.
2. Sims, P. A.; Larsen, T. M.; Poyner, R. R.; Cleland, W. W.; Reed, G. H. Reverse Protonation Is the Key to General Acid-Base Catalysis in Enolase. *Biochemistry* **2003**, *42* (27), 8298–8306.
3. Schreier, B.; Höcker, B. Engineering the Enolase Magnesium II Binding Site: Implications for Its Evolution. *Biochemistry* **2010**, *49* (35), 7582–7589.
4. Shen, T. Y.; Westhead, E. W. Divalent Cation and pH Dependent Primary Isotope Effects in the Enolase Reaction. *Biochemistry* **1973**, *12* (17), 3333–3337.
5. Poyner, R. R.; Cleland, W. W.; Reed, G. H. Role of Metal Ions in Catalysis by Enolase: an Ordered Kinetic Mechanism for a Single Substrate Enzyme. *Biochemistry* **2001**, *40* (27), 8009–8017.
6. Anderson, S. R.; Anderson, V. E.; Knowles, J. R. Primary and Secondary Kinetic Isotope Effects as Probes of the Mechanism of Yeast Enolase. *Biochemistry* **1994**, *33* (34), 10545–10555.
7. Schowen, B. S.; Schowen, R. L. [29] Solvent Isotope Effects on Enzyme Systems. *Meth. Enzymol.* **1982**, *87*, 551–606.
8. Pascal, B. D.; Willis, S.; Lauer, J. L.; Landgraf, R. R.; West, G. M.; Marciano, D.; Novick, S.; Goswami, D.; Chalmers, M. J.; Griffin, P. R. HDX Workbench: Software for the Analysis of H/D Exchange MS Data. *J. Am. Soc. Mass Spectrom.* **2012**, *23* (9), 1512–1521.
9. Gao, S.; Thompson, E. J.; Barrow, S. L.; Zhang, W.; Iavarone, A. T.; Klinman, J. P. Hydrogen Deuterium Exchange within Adenosine Deaminase, a TIM Barrel Hydrolase, Identifies Networks for Thermal Activation of Catalysis. *J. Am. Chem. Soc.* **2020**, *142* (47), 19936–19949.
10. Offenbacher, A. R.; Hu, S.; Poss, E. M.; Carr, C. A. M.; Scouras, A. D.; Prigozhin, D. M.; Iavarone, A. T.; Palla, A.; Alber, T.; Fraser, J. S.; Klinman, J. P. Hydrogen–Deuterium Exchange of Lipoygenase Uncovers a Relationship Between Distal, Solvent Exposed Protein Motions and the Thermal Activation Barrier for Catalytic Proton-Coupled Electron Tunneling. *ACS Cent. Sci.* **2017**, *3* (6), 570–579.
11. Waskom, M.; Botvinnik, O.; Hobson, P.; Cole, J. B.; Halchenko, Y.; Hoyer, S.; Miles, A.; Augspurger, T.; Yarkoni, T.; Megies, T.; Coelho, L. P.; Wehner, D.; cynddl; Ziegler, E.; diego0020; Zaytsev, Y. V.; Hoppe, T.; Seabold, S.; Cloud, P.; Koskinen, M.; Meyer, K.; Qalieh, A.; Allan, D. *Seaborn: v0.5.0 (November 2014)*, 0 ed.; 2014; p 12710.
12. Hunter, J. D. Matplotlib: a 2D Graphics Environment. *Computing in Science Engineering* **2007**, *9* (3), 90–95.
13. Zhang, J.; Balsbaugh, J. L.; Gao, S.; Ahn, N. G.; Klinman, J. P. Hydrogen Deuterium Exchange Defines Catalytically Linked Regions of Protein Flexibility in the Catechol O-Methyltransferase Reaction. *Proc. Natl. Acad. Sci. U.S.A.* **2020**, *117* (20), 10797–10805.